SLAC-PUB-2475
February 1980
(T/E)

THE PROBLEM OF R IN e^+e^- ANNIHILATION

R. Michael Barnett, Michael Dine and Larry McLerran
Stanford Linear Accelerator Center
Stanford University, Stanford, California 94305

ABSTRACT

A careful analysis is presented of the most recent data for $R(e^+e^- \to \text{hadrons})$ using improved theoretical techniques. The analysis is based on a generalized method for smoothing R. We show why the hadronic cross section is potentially one of the best tests of QCD. The theoretical complications such as unknown parameters and non-perturbative corrections are discussed, and resulting theoretical uncertainties are estimated. Some previously neglected QED corrections are accounted for. We find that for $\sqrt{s}$ near 7 GeV, the data lie about 15-17% above the theory; the experimental uncertainty is ±10% (dominated by systematics). For $\sqrt{s}$ near 5 GeV, the difference is only 5 - 8%. This apparent discrepancy may well be due to systematic problems in the experiment. For completeness we consider the possibility that there is a threshold for new particles at $\sqrt{s} \approx 6$ GeV. We consider new quarks, Higgs bosons, quixes, integrally-charged and even fractionally-charged leptons. While most of these hypotheses are not particularly attractive, some cannot be ruled out.

Submitted to Physical Review D

*Work supported by the Department of Energy, contract DE-AC03-76SF00515.

I. INTRODUCTION

The problem of finding convincing tests of quantum chromodynamics[1] (QCD) has proven to be difficult. However, as a result of the efforts to find such tests, many of the theoretical issues involved in comparing QCD with experiment are now better understood. The role of non-leading perturbative corrections, in particular, has received much attention recently.[2-4] It has become clear that order α_s^2 contributions must be computed if the theory is to be meaningfully tested and if the parameters of QCD are to be reliably determined.[2-6] It also appears that non-perturbative effects proportional to inverse powers of q^2 can complicate the analysis unless $|q^2|$ is quite large.[6]

In this paper, we will study the problem of testing QCD in the context of e^+e^- annihilation. In particular, we will consider the ratio

$$R \equiv \frac{\sigma(e^+e^- \to \text{hadrons})}{\sigma(e^+e^- \to \mu^+\mu^-)} \quad . \tag{1.1}$$

The second order QCD corrections to R have recently been computed,[4] and for center of mass energies $\sqrt{s} \gtrsim 3$ GeV, these corrections are quite small. This fact suggests that the predictions of QCD perturbation theory should be quite reliable. In addition, a thorough experimental analysis[7] has recently been completed of data[7] taken by the Stanford Linear Accelerator Center (SLAC)-Lawrence Berkeley Laboratory (LBL) collaboration with the Mark I detector at SPEAR (the "low-energy" e^+e^- storage ring at SLAC). New data are also being reported at higher energies at PETRA[8] (the high-energy e^+e^-

storage ring at the Deutsches Elektronen Synchrotron (DESY)). Here we will make a careful comparison of theory and experiment.

QCD is able to explain the successes of the parton model within a theory of strong interactions. At short distances, corrections to the quark-parton model can be computed systematically in powers of a small, running coupling constant $\alpha_s(Q^2)$ (where $\alpha_s(Q^2) \sim \log(Q^2/\Lambda^2)^{-1}$, and Λ is the scale parameter of QCD). These QCD corrections lead to scaling violations in many processes. A great deal of experimental and theoretical effort has been devoted to searching for such scaling violations. It is possible to study logarithmic scaling violations using leading-order QCD calculations. However, in order to reliably determine specific numbers such as α_s or cross sections, it is essential that the corrections beyond leading order in α_s be calculated.

We believe that e^+e^- annihilation is a particularly good context in which to examine QCD. The theoretical analysis of R in e^+e^- annihilation is conceptually extremely simple. At high energies and away from heavy quark thresholds there is only one relevant scale, the center of mass energy, $\sqrt{s}$. Unlike processes such as deep-inelastic scattering, where one needs to compile data over a range of Q^2 and x in order to observe a logarithmic deviation from scaling, one can consider a single number, the cross section at a fixed energy. Since this energy can be chosen to be quite large, one can hope to minimize non-perturbative effects, such as higher-twist terms, which plague analyses of deep-inelastic scattering. While at high energies the prediction for R is quite insensitive to the value of Λ, there is a measurable difference (of order 10%) between the prediction of QCD and of the quark-parton

model. Thus e^+e^- annihilation can be an outstanding test of QCD, though it is not likely to yield an accurate value for Λ.

In our comparison of theory and experiment we will consider a large number of possible corrections and uncertainties. For example, there are effects associated with quark masses, uncertainties about the application of QCD in the time-like region, and QED corrections. We will see that, after taking account of these effects, there is reasonable agreement between theory and experiment up to energies of 5.5 GeV. Above 5.5 GeV, a potentially serious discrepancy exists (about 15 - 17%). The theoretical prediction lies at the edge of the quoted systematic uncertainties (10%).[7] This potential discrepancy may well be due to real systematic problems in the experiment. It may, however, represent the presence of new phenomena in this energy range, or difficulties with QCD. We will consider these possibilities in the final sections of this paper.

The plan of this paper is as follows. In Section II, we briefly review the theoretical analysis of R in QCD. The perturbative results are summarized, and a variety of theoretical issues are considered. The problems associated with new quark thresholds and the inclusion of quark masses are described. We address as well the general problem of applying QCD in the time-like region. We describe our procedure for smoothing out the local fluctuations in R due to resonances and other, fundamentally non-perturbative, physics.

In Section III we consider certain QED corrections, pointed out by Yndurain,[9] which have been neglected in experimental analyses up to now. Inclusion of these corrections tends to improve agreement between theory and experiment. However, these corrections also enter the

determination of the luminosity. We estimate this effect, and find that it largely cancels the effect pointed out by Yndurain for present experiments.

In Section IV, we confront theory with data, with and without smoothing, and remark on the nature and magnitude of possible discrepancies.

Section V of this paper is devoted to the possibility that the apparent discrepancy between theory and experiment is due not to systematic error but to thresholds for new phenomena. Inclusion of an additional charge 1/3 quark is shown to give dramatic agreement with the data, but it is difficult to explain, in a conventional framework, why there are no corresponding narrow resonances. A new heavy lepton would give good agreement with the Mark I data for R, but other types of data may contradict such a hypothesis. The possibility that one or more scalar meson thresholds have been passed is shown to give marginal agreement with the data. Finally, we engage in some more exotic speculations.

In our final section we conclude with a discussion of some of the uncertainties which can affect the comparison of theory and data.

II. e^+e^- ANNIHILATION IN QCD

A. The theory of R

In the parton model, R simply measures the sum of the squares of the quark charges. In QCD, this value is approached asymptotically with increasing energy.[10] For massless quarks, R is infrared-finite order by order in perturbation theory. It is thus a function only of s and the renormalization scale μ. We can choose $\mu = s$; then R takes

the form

$$R = \sum_i Q_i^2 \left[1 + \frac{\alpha_s(s)}{\pi} + C_2 \left(\frac{\alpha_s(s)}{\pi} \right)^2 + \cdots \right] \quad . \qquad (2.1)$$

Here $\alpha_s(s)$ is the running coupling constant, and the sum runs over color and flavor. The coefficient C_2 has recently been calculated.[3] This constant cannot be specified without also specifying a renormalization procedure. The $\overline{\text{MS}}$ scheme of Bardeen et al.,[2] has been shown to yield small values for higher order corrections for both e^+e^- annihilation and deep inelastic scattering. In this scheme,

$$C_2 = 1.98 - 0.115\, n_f \qquad (2.2)$$

where n_f is the number of quark flavors. In determining R to second order, one must also include the second order corrections to the running coupling constant which appears in Eq. (2.1). Defining

$$\alpha_s^0(-q^2) = \frac{4\pi}{\beta_0 \ln(-q^2/\Lambda^2_{\overline{\text{MS}}})} \qquad (2.3)$$

where $\Lambda_{\overline{\text{MS}}}$ is a scale parameter to be determined from experiment and

$$\beta_0 = 11 - \frac{2}{3} n_f \quad , \qquad (2.4)$$

we use the Gell-Mann-Low equation[11] to write

$$\alpha_s(-q^2) = \alpha_s^0(-q^2)\left[1 + \frac{\beta_1}{4\pi\beta_0} \alpha_s^0(-q^2) \ln\ln(-q^2/\Lambda^2)\right] + \mathcal{O}\left[\left(\alpha_s^0(-q^2)\right)^3\right] \qquad (2.5)$$

For SU(3),[12]

$$\beta_1 = 102 - \frac{18}{3} n_f \qquad (2.6)$$

Fits to deep-inelastic scattering data give $\Lambda_{\overline{MS}} \approx 0.3$ GeV (within about 0.2 GeV).[13]

The calculation of R in e^+e^- annihilation treats the final state as if it consisted of free quarks and gluons. The effects which bind quarks into the observed hadrons are not directly taken into account. There are a number of arguments which make it seem reasonable to assume that these non-perturbative, confining effects are soft, and generate corrections to R which decrease rapidly with s.

One can be more rigorous and use dispersion theory to relate R(s) to the vacuum polarization amplitude evaluated at spacelike ($q^2 < 0$) momenta,[14]

$$\Pi_{\mu\nu}(q^2) = (q^2 g_{\mu\nu} - q_\mu q_\nu)\, \Pi(q^2) \quad . \tag{2.7}$$

This amplitude is related to the Fourier transform of the vacuum expectation value of the product of electromagnetic currents by

$$\Pi^{\mu\nu}(q) = \int d^4x\, e^{iq\cdot x} \langle 0|T\left(J^\mu(x)\, J^\nu(0)\right)|0\rangle \quad . \tag{2.8}$$

For q^2 large and negative, the right-hand side of this equation may be evaluated using Wilson's operator product expansion.[15] The usual perturbative analysis corresponds to evaluating the coefficient function for the leading-twist operator. The renormalization-group analysis for this term is given in Appendix A. Terms involving operators of higher dimension (higher twist) will fall off as powers of s relative to the perturbative contribution. One can try to estimate the contributions of non-leading twist operators by studying data at low s ($\sqrt{s} \sim 1$ GeV). Shifman et al.,[16] for example, have

attempted such an estimate. These contributions to R fall off as $1/s^2$ for large s, and can be ignored in the energy region considered in this paper.

In the case of massive quarks, one must exercise caution in applying the results of perturbation theory. The problem is most simply discussed in the time-like region. The diagram of Fig. 1 contains, near threshold, a velocity singularity characteristic of the Coulomb force. It diverges near threshold as v^{-1} where

$$v = \sqrt{\frac{s - 4m_Q^2}{s}} \quad . \tag{2.9}$$

These divergences become more severe in higher orders in perturbation theory. If the final-state particles were electrons, these diagrams would just sum to give the Balmer series for positronium, below threshold. Above threshold, they would give a Coulomb phase shift. In QCD, the bound state problem is inherently more complex, even within perturbation theory. In particular, new contributions to the long-range part of the force appear in every order, in contrast to QED, where only the lowest-order Coulomb force exists. These contributions will presumably be characterized by a coupling constant renormalized not at s but at the much smaller scales typical of bound state momentum transfers. Thus perturbation theory is unreliable near quark thresholds.

For energies well above threshold, mass corrections will fall as powers of m_Q^2/s. One can adopt a semiempirical approach to determine whether perturbation theory should be reliable. We expect that R will approach the perturbation theory results once the important bound

states channels have opened up and one is well into the continuum. Even well above threshold there are significant effects due to finite quark masses, which must be included in comparing theory and experiment. To deal with these contributions, we have used an "on-shell" definition of the quark mass. In first order in α_s, all the necessary information can be extracted from QED results (by including factors arising from color) and the first-order calculation of the β-function. To order α_s^2, the necessary calculations are not available, but since the mass effects are already small at order α_s, they should be negligible at order α_s^2.

For R we can write, using an interpolation formula due to Schwinger:[17]

$$R \approx \frac{1}{2} \sum_i v_i(3 - v_i)\, Q_i^2 \left[1 + \frac{4}{3}\, \alpha_s(s)\, f(v_i) + \frac{C_2}{\pi^2}\, \alpha_s^2(s)\right] \tag{2.10}$$

where

$$v_i = \sqrt{\frac{s - 4m_i^2}{s}} \tag{2.11}$$

and

$$f(v) = \frac{\pi}{2v} - \frac{3+v}{4}\left(\frac{\pi}{2} - \frac{3}{4\pi}\right) . \tag{2.12}$$

Here the sum runs over all quark flavors (and colors) with thresholds below s. The zeroth order term is the familiar parton model result. The 1/v term in f represents the Coulomb singularity described earlier. As remarked previously, as we approach thresholds, perturbation theory breaks down in two ways. First, additional singular terms (higher

powers of 1/v) appear in every order of perturbation theory; second, near threshold, the appropriate expansion parameter is $\alpha_s(p)$, where $p = m_q v$. Thus one can trust this expression for R only well away from thresholds or in appropriately smeared quantities (see Section II.B). Mass-dependent terms also appear in the running coupling constant. The following expression provides a reasonable approximation even below threshold,

$$\alpha_s(s) = \frac{12\pi}{33 \ln \frac{s}{\Lambda^2} - 2\sum_i \ln\left(\frac{s + 5m_i^2}{\Lambda + 5m_i^2}\right)} \quad . \tag{2.13}$$

In all of our work, we will treat the u, d and s quarks as massless. The mass-dependent terms will be kept only for the charm and heavier quarks.

B. The theory of smearing R

To apply the QCD calculation of R(s) to the experimentally measured R(s), we shall employ smearing techniques. These smearing techniques follow from the "optical theorem" which relates a suitably normalized vacuum polarization amplitude to R,

$$R(s) = \text{Im}\ \Pi(s) \quad . \tag{2.14}$$

This equation follows from Eq. (2.8) upon inserting a complete set of intermediate states between $J^\mu(x)$ and $J^\nu(0)$. This procedure also establishes $\Pi(s)$ as an analytic function of s with singularities only along the positive, real s axis.

The vacuum polarization amplitude is a function which is calculable in QCD. As discussed above, for values of s far from heavy quark thresholds, and for $|s|/\Lambda^2 >> 1$, a perturbative evaluation of $\Pi(s)$ should be valid. However, in the resonance regions the perturbative evaluation is not directly applicable and must be modified.

Among such modifications are dispersion theory techniques[14] which relate R to the vacuum polarization tensor for spacelike s, ($s < 0$). These techniques, however, are sensitive to data in the low-energy resonance region and in varying degrees to the unmeasured high-energy data. The interpretation of phenomena at a given energy is also obscure, since the dispersion relations involve relating $\Pi(s)$, for space-like s, to Π integrated over all time-like s ($s > 0$).

An alternative modification to the perturbative analysis was proposed by Poggio, Quinn and Weinberg.[18] They suggested using a variant of R which <u>can</u> be reliably calculated in perturbation theory. This variant, $\overline{R}$, is just a smoothed version of R. The data (and theory) for R(s) are convoluted with a function $W(s, s', \Delta)$ which produces a weighted average of the data in the interval $(s-\Delta) \lesssim s' \lesssim (s+\Delta)$. Δ is chosen so as to smooth out the resonant structure.

In our analysis, we will use a slightly more general version of the smearing method introduced by Poggio, Quinn and Weinberg. We define the smeared $\overline{R}$ as

$$\overline{R}(s) = \int_{4m_\pi^2}^{\infty} ds' \, W(s, s', \Delta) \, R(s') \quad . \tag{2.15}$$

An example of W is

$$W(s, s', \Delta) = e^{-\frac{1}{2}(s-s')^2/\Delta^2} \quad . \tag{2.16}$$

The smearing function W used by Poggio, Quinn and Weinberg was

$$W(s, s', \Delta) \propto \frac{1}{(s-s')^2 + \Delta^2} \quad . \tag{2.17}$$

We shall now show that if W is an analytic function of s and s' with no singularity within a distance Δ of the positive real axis, then $\overline{R}$ may be evaluated in perturbation theory. (The parameter appropriate for this expansion is $\alpha_s(\Delta)$). To see this we use the "optical theorem" of Eq. (2.14) to derive a contour integral representation for $\overline{R}$. Using Eqs. (2.14) and (2.15) we have

$$\overline{R}(s) = \int_{4m_\pi^2}^{\infty} ds' \; W(s, s', \Delta) \; \mathrm{Im}\, \Pi(s') \quad , \tag{2.18}$$

which can also be written as

$$\overline{R}(s) = \int_C \frac{ds'}{2i} W(s, s', \Delta) \; \Pi(s') \quad . \tag{2.19}$$

The contour C is shown in Fig. 2.

To show that $\overline{R}$ may be evaluated perturbatively, we deform the contour of Eq. (2.19) to the contour C' shown in Fig. 3. For values of s' along the contour C', we may expand Π in perturbation theory. For values of s far from quark thresholds, and for $|s|/\Lambda^2 \gg 1$, the expansion parameter is $\alpha_s(|s|/\Lambda^2)$. Near a heavy quark production

threshold, however, the expansion parameter is $\alpha_s(\Delta/\Lambda^2)$. Although unsmeared perturbation theory would break down, the smearing procedure removes singularities from the perturbation expansion (for Δ/Λ^2 sufficiently large), and therefore $\overline{R}$ may be evaluated in perturbation theory. These singularities would reappear as $\Delta \to 0$, and perturbation theory would again break down. (For s near zero, that is, in the resonance region for low mass quarks, these same arguments hold.)

III. QED CORRECTIONS

Theoretical expressions for R are generally obtained in the one-photon approximation. However, certain QED corrections which are nominally higher order in α (the fine structure constant) can be comparable to QCD corrections at high energies and must be carefully taken into account. Bremsstrahlung from the electron or positron line, as well as contamination from the two photon processes, are accounted for in the experimental analyses. Other QED corrections are also substantial at SPEAR energies. In particular, diagrams with a vacuum polarization insertion on the photon line (Fig. 4) can be quite large.[9] As an example, consider the diagram with an electron loop shown in Fig. 5. This diagram contains a term $(\alpha/3\pi)\ \ell n(s/m_e^2)$. For $\sqrt{s}$ = 3 GeV, the logarithm is 17.4. Thus, when this amplitude is interfered with the Born term (Fig. 6), it gives a 3% contribution to the cross section.

For the μ-pair and hadron production cross sections, these corrections correspond to replacing α by $\alpha(s)$, the running coupling constant of QED, in computing the Born term. Thus if one compared the measured hadronic cross section with the measured μ-pair cross section, such effects would cancel out. It is important to note, however, that

the quoted value for R is a corrected hadronic cross section divided by the theoretical point cross section for $\mu^+\mu^-$ production. For the analysis at Mark I, only loops of electrons were included in the corrections. As Yndurain has pointed out,[9] however, the other contributions to vacuum polarization give a three to four percent contribution at these energies. Since QCD corrections to the parton model relations are only of order 10%, it is important to include these effects.

However, such corrections also play a role in the determination of the luminosity of the storage ring. The luminosity is determined by measuring the Bhabha cross section (Fig. 7). At SPEAR (as in many experiments), these measurements are made at wide angles;[7] they thus involve large momentum transfers. For these momentum transfers, the vacuum polarization corrections are again large. The luminosity is determined by comparing the measured Bhabha rate with a theoretical expression for the cross section. Once more, this theoretical expression includes only the Born term plus electron loop corrections to the virtual photon line. As discussed below, the inclusion of the contributions of other particles to the vacuum polarization largely cancels out the effect noted by Yndurain.

Most of the ingredients necessary for the analysis have been presented[9] by Berends and Komen and by Yndurain, and we review these briefly here. The real part of the vacuum polarization tensor is easily computed for leptons. The contribution of each is given by the formula,

$$\text{Re } \Pi(s) = -\frac{2\alpha}{3\pi} Q^2 V(s) \quad , \qquad (3.1)$$

where

$$V(s) = \frac{5}{3} + \frac{4m^2}{s} + 2\left(1 - \frac{4m^2}{s}\right)\left(1 + \frac{2m^2}{s}\right) X(s) \quad , \tag{3.2}$$

Q and m are the charge and mass of the lepton, respectively,

$$\begin{aligned} X(s) &= \frac{1}{2v} \ln \left| \frac{1-v}{1+v} \right| \quad , \quad s \geq 4m^2 \\ &= \frac{1}{v} \tan^{-1}\left(\frac{1}{v}\right) \quad , \quad 0 \leq s \leq 4m^2 \quad , \end{aligned} \tag{3.3}$$

and

$$v = \sqrt{\left| \frac{s - 4m^2}{s} \right|} \quad . \tag{3.4}$$

The hadronic contribution to Π can be obtained from experimental data using the dispersion relation,

$$\text{Re } \Pi_h(s) = \frac{s}{4\pi^2 \alpha} \int_{4m_\pi^2}^{\infty} \frac{\sigma(s')}{s' - s} \, ds' \quad . \tag{3.5}$$

The integral on the right hand side has been estimated by Berends and Komen and by Yndurain for several values of s, and they obtain similar results.

For our analysis of the hadronic contribution, we used the naive QCD expression

$$\text{Re } \Pi_h(s) = -\frac{2\alpha}{3\pi} \sum_i Q_i^2 \, V_i(s) \left[1 + \frac{\alpha_s\left(\frac{s}{\Lambda^2}\right)}{\pi} \ln \ln \left(\frac{|s|}{m_i^2} \right) \right] \quad , \tag{3.6}$$

and determined the m_i for light quarks by fitting to results given by Berends and Komen. The sum here is over quark flavors (and colors).

Taking

$$\begin{aligned} m_u &= m_d = 0.1 \text{ GeV} \\ m_s &= 0.4 \text{ GeV} \\ m_c &= 1.25 \text{ Gev} \\ m_b &= 4.7 \text{ GeV} \end{aligned} \tag{3.7}$$

we obtained agreement to a few percent over the energy range of interest. The resulting uncertainty in the cross section is less than 0.05%.

The corresponding corrections to the Bhabha cross section are computed from the diagrams of Fig. 7, in terms of Re $\Pi(s)$. Denoting the change in the differential cross section by $\delta(d\sigma/d\Omega)$, we have

$$\delta \frac{d\sigma}{d\Omega} = -\frac{\alpha^2}{s\psi^2} \{(2 - 2\psi + \psi^2) \text{ Re } \Pi(t) - \psi(1-\psi)^2 [\text{Re } \Pi(t) + \text{Re } \Pi(s)]$$

$$+ \psi^2(1 - 2\psi + 2\psi^2) \text{ Re } \Pi(s)\} \quad . \tag{3.8}$$

Here $\psi = \sin^2(\theta/2)$, $z = -s\psi$ and θ is the angle relative to the beam direction.

To correct the Mark I data, we integrated this expression over the angular range used in the luminosity determination for various values of s. Again, we included the effects of muons, τ-leptons and hadrons, all of which had been neglected in the experimental analysis.

The effect of including these corrections is largely to cancel out the correction to the hadronic cross section. The remaining

correction is never more than half a percent over the energy range of interest. This result is easily understood. The vacuum polarization corrections may be thought of as building up the running coupling constant of QED. Including them in the hadronic cross section is equivalent to replacing α by $\alpha(s)$ in the Born term. Similarly, in the Bhabha cross section, α is replaced by $\alpha(s)$ in the s-channel diagram, and by $\alpha(t)$ in the t-channel diagram. Since the Bhabha measurement is performed at large angles, s is of the same order as t. Then $\alpha(s) \sim \alpha(|t|)$, to logarithmic accuracy. For completeness, these corrections have been retained in all the curves shown in this paper.

IV. COMPARISON OF THEORY AND DATA

A. Data

We consider here the most recent compilation of data[7] for R taken with the Mark I detector by the SLAC-LBL collaborations. Because there may be 10 - 15% overall normalization differences between the R data sets of different experiments, we have restricted our analysis to the SLAC-LBL (Mark I) data. This data set (unlike all others) includes significant coverage of the region between $\sqrt{s}$ = 5 and 8 GeV, which is of particular interest to us. For comparison purposes, we will display the world's data on one plot.

We have used a fine grid of 147 data points from $\sqrt{s}$ = 2.6 to 7.8 GeV, with the highest density of points in the resonance region ($\sqrt{s} \approx$ 3.7 to 4.5 GeV). The J/ψ and ψ' are included (as they must be for the integrals described below). For graphical purposes, we use larger bins in order to reduce the number of data points. The error bars shown are for statistical errors only. There is a 10%

systematic uncertainty in the overall normalization. There may be a point-to-point systematic error of about 3% for every 0.5 GeV interval.

The contribution to R of the tau lepton has been subtracted from the SLAC-LBL data. The data are also corrected for the two-photon component of the cross section; this is a small correction ($\sim 2\%$) because of experimental cuts. The QED radiative corrections from bremsstrahlung have been accounted for.

One must be sure that one is comparing the identical quantities for theory and experiment. There has been confusion in the past for several reasons. First, the muon cross section used in obtaining the value of R quoted by experimentalists is the theoretical, point cross section, $\sigma(e^+e^- \to \mu^+\mu^-)$. Second, in the numerator $[\sigma(e^+e^- \to \text{hadrons})]$, the electron vacuum polarization term (see Fig. 5) has been subtracted, but the muon, tau and hadronic contributions have not been subtracted.[9] As discussed in Section III, these corrections can be numerically significant at SPEAR energies. Third, the numerator is normalized to the measured Bhabha ($e^+e^- \to e^+e^-$) cross section at large angles; in this normalization the theoretical Bhabha cross section is taken to be the point cross section, again with corrections only for electron vacuum polarization. It follows that the quoted R is given by

$$R_e = \frac{(\sigma_h^{\text{measured}} - \sigma_h^e)}{\sigma_\mu^0} \kappa \tag{4.1}$$

where

$$\kappa = \frac{\delta_e^0 + \delta_e^e}{\delta_e^0 + \delta_e^e + \delta_e^\mu + \delta_e^\tau + \delta_e^q} \tag{4.2}$$

$$\sigma_h^{\text{measured}} - \sigma_h^e = \sigma_h^0 + \sigma_h^\mu + \sigma_h^\tau + \sigma_h^q \qquad (4.3)$$

$$\delta_e^{\text{measured}} - \delta_e^e = \delta_e^0 + \delta_e^\mu + \delta_e^\tau + \delta_e^q \quad . \qquad (4.4)$$

σ_h^i and σ_μ^i refer to the total cross sections into hadrons and into muons. δ_e^i refers to the Bhabha cross section into the solid angle covered by a given detector. The superscript 0 on σ and δ refers to the point cross sections while the superscripts e, μ, τ and q refer to the interference terms involving e, μ, τ and quarks in vacuum polarization loops (as in Fig. 5). $\sigma_h^{\text{measured}}$ and $\sigma_e^{\text{measured}}$ are the measured cross sections with bremsstrahlung radiative corrections included.

B. Theory

The theoretical curves used in comparisons with data resulted from QCD calculations of R with α_s and α_s^2 terms included. For a given value of Λ, the magnitude of the α_s^2 term depends on the renormalization scheme and on the definition of the correction term in α_s itself. We have used the $\overline{\text{MS}}$ renormalization scheme of Bardeen et al.,[2] and

$$\alpha_s(Q^2) = \alpha_s^0(Q^2) - \left(\alpha_s^0(Q^2)\right)^2 \frac{\beta_1}{4\pi\beta_0} \ell n \ell n(Q^2/\Lambda^2) \quad . \qquad (4.5)$$

In general the α_s^2 term in R is only about 1% of the total, as expected.

The value of m_c used was obtained in the smoothing procedure (described below) and reflects the inclusion of J/ψ and ψ'. The results are not very sensitive to the value chosen for Λ; for comparison we will plot curves for $\Lambda = 200$, 450 and 700 MeV. We have not included the

contributions of the weak interactions, since they are negligible in the region of interest. For $\sqrt{s} \leq 30$ GeV, they contribute less than 0.01 units of R, while at $\sqrt{s} = 40$ GeV they add 0.08 units of R.

Since the QED radiative corrections for vacuum polarization loops with muons, taus and hadrons have not been subtracted from the SLAC-LBL (Mark I) data, we have added them to the theoretical calculations. These corrections enter in two places: in the hadron cross section and in the Bhabha cross section which is used to normalize the hadron cross section (see Eqs. (4.1) and (4.2)). The corrections to each of the two cross sections are about 3% separately, but they tend to cancel, resulting in corrections of about 0.5%.

C. Comparison of raw theory and data

In Figs. 8 and 9, the data and theory are shown. Figure 9 shows all data available as of August 1979 except in the $\sqrt{s} = 3.7 - 4.7$ GeV (resonance) region. Our attention will focus on Fig. 8 showing the SLAC-LBL (Mark I) data. Of particular interest to us is the region from $\sqrt{s} = 5$ to 8 GeV which is far from both the c and b quark thresholds. Theory and data appear to be in reasonably good agreement around $\sqrt{s} = 5$ GeV, but the QCD curves fall consistently below the data for $\sqrt{s} = 5.5$ GeV. The significance of this discrepancy will be analyzed following the discussion of the smearing procedure. It can be seen that the results are relatively insensitive to Λ for larger values of $\sqrt{s}$.

D. Smeared theory and data

The theory behind the smearing procedure has been discussed in Section II.B. We have compared the results of several different

weighting functions. In each case the theory and the data are smeared with the same weighting function. Two of these functions are (with $s = 4E^2$):

$$W_{ij} = [(s_i - s_j)^2 + \Delta^2]^{-1} \quad , \tag{4.6}$$

(of Ref. 18) and

$$W_{ij} = \exp[-\tfrac{1}{2}(s - s')^2/\Delta^2] \quad , \tag{4.7}$$

where the smeared $R \equiv \overline{R}$ is

$$\overline{R}(s_i) = \frac{\sum_j R(s_j)\, W_{ij} \left(\frac{s_{i+1} - s_{i-1}}{2} \right)}{\sum_j W_{ij} \left(\frac{s_{i+1} - s_{i-1}}{2} \right)} \quad . \tag{4.8}$$

For both theory and data, the s_j are chosen only where data exist (except for $\sqrt{s} < 2.5$ GeV and $\sqrt{s} > 7.9$ GeV). Since the smearing procedure requires integrating (summing) over all s, we assign the value $R = 2.5 \pm 2.5$ for points with $\sqrt{s} < 2.5$ GeV and $R = 4.3 \pm 4.3$ for $\sqrt{s} > 7.9$ GeV; since these error bars are clearly exaggerated, the resulting error bars on the smoothed data are also exaggerated. For the bin including the J/ψ (and similarly for the ψ', T and T') we have assigned a value to R such that the integral over the bin gives the experimentally determined integrated contribution[19] to R (plus background). In particular

$$R_{res} \sim \frac{\Gamma_{ee}}{\Delta E} \frac{\Gamma_{had}}{\Gamma_{all}} + \text{background} \sim \frac{\Sigma_{had} m^2}{\Delta E} + \text{background} \tag{4.9}$$

where Σ_{had} is the integrated cross section to hadrons.

The results from smearing with the two weighting functions are shown in Fig. 11. The error bars (which are obtained by the standard procedure for statistical errors) vary according to function, but the relative shapes of smoothed theory and smoothed data are not significantly different for different weighting functions.

Here we concentrate on results obtained with the Gaussian weighting function (Eq. 4.7). The results of smearing with this function for different values of Λ are shown in Fig. 11. It is evident that below $\sqrt{s}$ = 5.5 GeV and above the charm threshold region, there is good agreement between the predictions of QCD and the SLAC-LBL (Mark I) data. There is only a small (5 - 8%) discrepancy in the relative normalizations. However, between $\sqrt{s}$ = 5.5 and 7.8 GeV, there is a significant difference between the predictions of QCD (with u,d,s,c and b quarks) and the data. This difference is about 15 - 17% and is far greater than allowed by statistics, but is at the edge of the limits set by systematic errors (which are ±10%).[20] The rise of the data between $\sqrt{s}$ = 5.5 and 6.5 GeV is also at the limit of the estimated energy-dependent systematic errors.[20] If future experiments are able to decrease the systematic errors, then this discrepancy would become a significant problem.

V. EFFECTS OF ADDITIONAL THRESHOLDS

Examination of Fig. 11 reveals a potential discrepancy between theory and experiment. We feel that the magnitude of this discrepancy is not large enough to demand consideration of additional thresholds. It is interesting nonetheless to note the impact of various hypothetical particle thresholds on the theoretical predictions, since it is

possible that future experiments might give credence to the discrepancy. It is conceivable that there are new particles of mass 2 - 3 GeV which have been overlooked.

The effect of a quark of charge -1/3 and mass 3 GeV (compared with $m_c = 1.38$ GeV) is shown in Fig. 12. The resulting theoretical curve appears to be in excellent agreement with the data except for a slight (6 - 7%) overall normalization difference. To eliminate the question of normalization, we can consider the slope of R as in Fig. 13.

Given our knowledge about ψ and Υ, it is easy to estimate the magnitude of Γ_{ee} for the $q\bar{q}$ resonance expected for such a new quark ($\Gamma_{ee} \approx 1$ keV). However, the Mark I detector has scanned very carefully through the region $\sqrt{s} = 4.5$ to 7.5 GeV and such resonances have apparently been ruled out, $\Gamma_{ee} \lesssim 0.15$ keV at the 90% confidence level.[21] If this resonance, unlike ψ and Υ is very wide ($\gtrsim 100$ MeV) then it might well have been missed. Such a width would require an entirely different decay mechanism than that which operates in the ψ and Υ systems. Note that results from high energy machines ($\sqrt{s} > 10$ GeV) cannot easily rule out this hypothesis; because of systematic errors in normalization, it would be necessary to go down to $\sqrt{s} \approx 5.5$ GeV and observe the threshold region for such a quark. So it is improved experiments at SPEAR energies which are needed.

Since the primary problem with proposing a new quark is that the associated resonances have not been observed, one should consider the possibility of a new lepton of mass ≈ 2.9 GeV. As seen in Fig. 14, even the full contribution of an integrally-charged lepton is allowed by the Mark I data. An additional full unit of R would appear to be

ruled out at $\sqrt{s} \approx 30$ GeV by data from PETRA[8] (see Fig. 9), but one should remember that the experimental cuts used in determining R at PETRA are quite different than those used at SPEAR. In particular, PETRA experiments typically require $E_{visible} \gtrsim 0.50\ E_{total}$ compared with $\gtrsim 0.20\ E_{total}$ at SPEAR. The 2-prong signal used for identification of τ is also relevant to identification of a new heavy lepton. The Mark I data[22] for 2-charged-prong events (with the τ background subtracted and prong $\equiv$ e,μ or hadron) can be interpreted as showing that the 2-prong rate increases after $\sqrt{s} \approx 5.5$, but this may not be significant because of low efficiency. The 2-prong (e + X) data[23] from the DELCO experiment at SPEAR are between 20% and 50% higher than expected from τ for $\sqrt{s} = 6 - 8$ GeV. On the other hand the Mark J data (μ + X) of Ref. 24 at $\sqrt{s} \geq 13$ GeV and the Mark I data[22] for μ + e events at $\sqrt{s} = 6 - 8$ GeV appear to allow a new contribution which is no more than 30 - 40% of that due to the τ. Another signal which might be relevant at PETRA energies is that of events with 1 prong in one hemisphere and 3 prongs in the other.

A conventional lepton which decayed into a massless neutrino (plus anything) would contribute to R at SPEAR but would not contribute to R at PETRA because of the visible-energy cut. Because of the presence of additional decay channels ($\bar{c}s$ and $\bar{\nu}\tau$), the 2-prong signal would occur approximately 50% as often as for τ. This appears to be slightly more than allowed by the data of Ref. 24, but this and the "1 prong + 3 prongs" mode should be subjected to further experimental scrutiny. If the new heavy lepton decays instead into a massive ($\sim$2 GeV) stable neutrino, then the 1 + 3 prong mode would decrease and the 2-prong mode would be

similar to that for τ. However, the two prongs would each have very little energy ($\sim$2 GeV) and some experiments might exclude such events. A lepton which decays into massive, stable neutrinos would contribute to R at SPEAR but not at PETRA. If the massive neutrino were not stable, then conclusions depend on the decay modes assumed. If the dominant decay was to τ (plus anything) then few 2-prong or 1 + 3 prong events might appear. However, there would probably be a significant contribution to R at PETRA. Depending on visible-energy cuts (and other cuts) there could be more or less than half a unit of R (see Fig. 9). One could also consider more exotic decay modes of the charged and neutral leptons.

One might also speculate on the existence of new spin 1/2 leptons of fractional charge (we use the work "lepton" to indicate the absence of strong interactions). A lepton of charge 2/3 and mass 3 GeV, or a degenerate multiplet of charge -1/3 leptons, would give almost the same excellent fit as in Fig. 12. These new leptons must be short-lived. Long-lived particles of charge 2/3 would have been identified as fractionally-charged particles by the Mark I and other detectors. Long-lived particles of charge -1/3 would most likely escape detection at all present detectors, and therefore would not contribute to R. If, however, leptons of charge 2/3 or -1/3 decayed into a charge -1/3 lepton (of mass 1 - 2 GeV?) plus integrally-charged particles, then the events would contribute to R and the outgoing charge -1/3 lepton would most likely escape detection. We conclude from our discussions with experimentalists that while it is dubious that any present accelerator

experiment would observe leptons of charge -1/3, experiments such as FQS (at PEP), JADE (at PETRA) and Crystal Ball (at SPEAR) should be able to find such a particle within half a year (if it exists).

A necessary consequence of this proposal is that at least one of the final products must be a stable, fractionally-charged particle which should be found free in nature. One experiment has reported observing fractionally-charged particles residing in matter,[25] but nothing is known about their masses or interactions.

Let us return to the possibility that the resonances associated with a new quark are not observed because they are quite wide. There are a number of speculative mechanisms which might broaden otherwise narrow resonances. One could, for example, imagine that these new quarks are subject to some new, very strong interactions. One could also consider the possibility that these quarks transform according to some larger representation of the color group than the three (possibly with some new charge assignment). The existence of such quarks has been suggested before in other contexts. In particular, the possibility that these quarks transform as sixes (quixes) have been considered by several authors.[26] These authors considered the possible weak interactions of such particles, and explained why they might have escaped detection in stable particle searches. While others have not considered quixes in our context, quixes could be relevant since a charge -1/3 quix would contribute 2/3 units of R. This is near the upper limit of what one could tolerate to explain the data. However, the widths of the associated resonances would be only about fifty times larger than those of ordinary heavy quarks, which is not broad

enough to hide them from narrow resonance searches. One can consider other representation and charge assignments, but these usually suffer from similar problems and in any case are aesthetically unpleasing.

Another possible explanation for the apparent rise in R is that pairs of charged scalar (Higgs) bosons[27] are produced. This production would contribute 1/4 units of R far above threshold. However, near threshold, this contribution would rise quite slowly with s compared with quark production. e^+e^- annihilation occurs through a spin-1 channel and, as a result, scalars must emerge in a P-wave. Fermions, on the other hand, may be produced in an S-wave. As a result, scalar production near threshold is suppressed by a factor of v^2 ($v \equiv$ velocity, Eq. (2.9)) relative to quark production. While scalar bosons might account for the magnitude of the discrepancy in R, they cannot explain the apparent threshold visible in Fig. 11 near $\sqrt{s} = 5.5$ GeV. Since one scalar boson gives a very small contribution, we have assumed in Fig. 15 that there are two scalar bosons of mass = 2 GeV. Such bosons would probably be difficult to observe.

Other possibilities are even more speculative. One might imagine that the charm quark has some structure on a scale of a few GeV, and that its production should be described by a form factor. This seems unlikely, since we have no evidence that e, μ and τ leptons or u, d and s quarks possess structure at such scales. Nonetheless, one can fit the data in this fashion. One could assume that the form factor occurs because the charm quark is composite with constituent masses of order 3 GeV. There are at least three new parameters (the scale of the form factor, the mass of the constituents and the magnitude of their

contribution) so it is very easy to obtain excellent fits as in Fig. 16. Given the number of parameters, however, the quality of the fit does not provide motivation for this hypothesis.

As we have remarked before, the data do not necessarily require hypotheses of the type we have described, because of the large systematic uncertainties. Moreover, none of the ideas we have considered seem particularly attractive. Nonetheless we feel it is worthwhile to keep in mind that there remains the possibility that new phenomena exist at what are now referred to as "low energies".

VI. CONCLUSIONS

In the previous sections, we have compared theory and experiment in e^+e^- annihilation. We have noted that there may be a discrepancy between the predictions of QCD and the values of R determined by the SLAC-LBL collaboration. A variety of explanations for this apparent discrepancy have been considered. Unfortunately, none of the explanations which we have proposed seem particularly appealing. As we conclude, it is perhaps worthwhile to review the uncertainties which enter into the theoretical determination of R, and to present them in tabular form.

These uncertainties fall into three classes. First, the numerical parameters which enter into QCD calculations (coupling constant, masses) are only approximately known. Second, the magnitude of higher-order, uncalculated QCD (and QED) corrections are unknown. Finally, one must worry about possible non-perturbative effects.

The numerical quantities which parametrize QCD are the scale parameter, Λ, which characterizes the running coupling constant, α_s, and the quark masses, m_q. Much effort has been devoted to extracting Λ from deep-inelastic scattering data. As in the case of e^+e^- annihilation, theoretical contributions through second order in α_s must be kept, and (in comparisons) one must use the same renormalization scheme as for e^+e^- (here the $\overline{MS}$ scheme of Bardeen et al.[2]). However, there are uncertainties (beyond experimental ones) in the value of Λ, since this value is dependent on the method of extraction and on the possible presence of significant higher-twist corrections.[6] As a result (if we are very conservative), Λ may not be known to better than $\pm$ 200 MeV (with Λ probably less than 400 MeV). This uncertainty in Λ leads to an uncertainty in R of about 2% for $\sqrt{s}$ = 5 - 7 GeV. Precision deep-inelastic scattering experiments now in progress will decrease the uncertainty somewhat.

This uncertainty is quite small compared to the systematic errors of typical experiments which measure R (10 - 15%). Thus it is unlikely that even greatly improved e^+e^- measurements will give a better determination of Λ than that provided by current deep-inelastic scattering experiments. However, such experiments <u>can</u> hope to measure deviations from scaling. The difference between the parton model and QCD predictions are of order 10% in the energy range considered in this paper.

Uncertainties in the numerical values of quark masses are important only for energies near quark thresholds. For the energy region considered in our analysis, only uncertainties in the charmed-quark mass are important. The mass itself is quite accurately determined

by matching the energy of the theoretical rise in R due to production of charmed quark with the experimental rise. In this paper we have used an on-shell definition of the quark mass. This mass was determined by matching the threshold behaviour of the theoretical and experimental curves for $\overline{R}(\Delta,s)$. The uncertainty in the value of the charmed quark mass obtained in this way was of order 5%. While the corresponding uncertainty in $\overline{R}$ may be as large as 10% near threshold ($\sqrt{s} \approx 3$ GeV) it is less than 0.1% for $\sqrt{s} \gtrsim 4.1$ GeV.

The expectation for the theoretical value for R is, of course, subject to uncertainties due to the perturbative contributions of higher order which have not been calculated. These can arise from both QCD and QED. The QCD calculations are naturally divided into two distinct energy regions: energies far from quark thresholds, and energies within 1 - 2 GeV of a new quark threshold.

Near a quark threshold, we have argued the appropriate expansion parameter is roughly $\alpha_s(\Delta)$, where Δ is the smearing parameter. Since mass corrections have only been calculated through order α_s, we expect uncalculated perturbative contributions to be of order $3\left(\alpha_s(\Delta)\right)^2 Q_i^2$, where Q_i^2 is the charge of the "new" quark. For the charmed quark and values of Δ of order 5 GeV^2, this number is of order 0.2, or about 5% of R very near threshold.

Away from quark thresholds, we expect the theoretical calculation to err by an amount of order $\alpha_s^3(s)$. In processes in the time-like region, one frequently finds larger corrections. In Drell-Yan proceses, for example, second order corrections are comparable in magnitude to

the first order corrections.[28] Moorhouse, Pennington and Ross[29] have studied this problem in e^+e^- annihilation. The corrections which they considered can be included by carefully taking the discontinuity of the renormalization-group-improved expression for $\alpha_s(-q^2)$. At 5 GeV they are of order 1%, and tend to decrease the value of R. We expect the sum total of effects in order $\alpha_s^3(s)$ to be 1 - 2%.

QED corrections of order $(\alpha/\pi)^2$ which have not yet been calculated will give contributions to R which are small compared to the second-order QCD contribution. We expect these corrections to make at most a 0.2% contribution to R.

Among the uncertainties which arise from non-perturbative effects are those due to thresholds for new, exclusive channels. For example, one may well ask whether the rise in R near $\sqrt{s}$ = 5.5 - 6 GeV might be due to a threshold for the production of charmed baryons. We believe this explanation is implausible since this rise begins at an energy well above the threshold for production of charmed baryons. The measured rise of charmed-baryon production[30] begins at $\sqrt{s} \approx 4.5$ GeV and levels off at about $\sqrt{s}$ = 5.1 GeV. The more general question of whether, far from the threshold for the production of a new species of quarks, the opening of new exclusive channels affects R significantly can only be answered by considering the concept of local duality. We address this question below.

It is quite reasonable to think that we can calculate quantities such as $\Pi(q^2)$ in the deep Euclidean region. Quantities relating to the time-like region, on the other hand, involve inherently non-perturbative phenomena. We have at best a limited understanding of

the manner in which quarks "evolve" into observed hadrons. The comparison of the unsmeared R with data away from resonance regions relies on the hope that these non-perturbative effects are soft, and have little effect on the total cross section.

In applying smearing techniques or dispersion relations, however, we are relying on much weaker assumptions. Essentially, all we are assuming is that $\Pi(q^2)$ is a smooth function away from the real, positive q^2 axis. The smoothness assumption is almost equivalent to the assumption of local duality. Consider, for example, the heavy-quark resonance regions. If the cross section is smeared over an interval Δ much larger than the spacing and widths of the resonances, we expect that the result should be insensitive to the detailed resonant structure. This will certainly be true, as we say in the discussion of Section II.B, if $\Pi(q^2)$ is sufficiently smooth at a distance Δ from the real axis.

The arguments of Section II.B also require that $\Pi(q^2)$ behave sufficiently well at infinity that the relevant integral converge. Of course, at high energies $\Pi(q^2)$ is determined by unknown physics, but it would be surprising if the high-energy behavior were so bad as to destroy the smearing arguments.

Some notion of the validity of the smearing arguments can be obtained by comparing the results obtained from theory and experiment with different smearing functions. This tests the "smoothness" hypothesis implicit in the smearing procedure, as well as the importance of unmeasured high-energy data to the comparison of theory and experiment. It is particularly useful to compare the power-law type smearing with the exponential smearing we have proposed in this paper.

The exponential smearing function gives less weight to high-energy behavior than the power-law smearing functions; in fact, high-energy behavior cannot significantly alter the results obtained with exponential weighting. On the other hand, the validity of exponential weighting requires smoother behavior for $\Pi(q^2)$ in the complex plane than power law weighting. It is reassuring, then, that the difference between theory and experiment obtained using the smearing function of Poggio, Quinn and Weinberg[18] and the difference obtained with the Gaussian weight of Eq. (2.16) differ by only about 1% in the entire energy range. The conclusions were similar with other smearing functions.

Certain non-perturbative effects can be treated more quantitatively. Several authors have considered the effects of operators of higher twist generated by low-mass quarks and the effects of instantons. Instantons appear to give contributions which fall off as very large powers of s.[31] Both of these effects are negligible at high energies. Near thresholds for production of heavy quarks, additional higher-twist effects occur[32] associated with the inverse velocity contributions to R (see Eq. 2.10 and the discussion below it). The resulting uncertainties can be estimated using the local duality arguments discussed above. We find that such contributions should be negligible for energies which are 1 - 2 GeV above the $\sqrt{s} \approx 3$ GeV charm threshold and less than 5% very near threshold.

Now we summarize the results of this section in Table I.

ACKNOWLEDGMENTS

We thank J. Bjorken, D. Coyne, S. Drell, G. Feldman, C. -S. Gao, F. Gilman, A. Guth, T. Huang, G. Kane, I. Karliner, J. Kirkby, V. Luth, M. Perl, H. Quinn, F. Rosner, J. Sapirstein, R. Schwitters, J. Siegrist and T. Walsh for interesting and enlightening discussions. This paper was supported by the Department of Energy under contract number DE-AC03-76SF00515.

APPENDIX

RENORMALIZATION GROUP FOR $\Pi(q^2)$

$\Pi(q^2)$ is not multiplicatively renormalized. Its divergences, which are associated with the wave function renormalization of the photon, are cured by subtraction. The renormalization group analysis of $\Pi(q^2)$ is particularly simple if 't Hooft's minimal subtraction scheme is used.[33] In this scheme, one first computes the appropriate Feynman diagrams (Fig. 17) using the dimensional regularization procedure of 't Hooft and Veltman.[34] Here Feynman diagrams are continued to 4-ε dimensions, and ultraviolet divergences appear as poles in ε. The bare coupling has dimension

$$g_0 \sim m^{\varepsilon/2} \quad . \tag{A.1}$$

To keep the renormalized coupling constant dimensionless, one writes

$$g = \mu^{-\varepsilon/2} Z_g g_0 \quad , \tag{A.2}$$

where μ is an arbitrary mass and Z_g is an appropriate (dimensionless) combination of wave function and vertex counterterms. These counterterms are chosen to cancel only the poles in ε. In this appendix the quark masses m_i, are renormalized according to the same prescription. (The "on-shell" procedure used in the text is discussed briefly at the end of this section.) Thus for Π we have

$$\Pi(q^2,g^2,m^2,\mu) = \Pi_0(q^2,g_0^2,m_0^2,\varepsilon) - \mu^{-\varepsilon} \sum_{n=1}^{\infty} \frac{C_n(g)}{\varepsilon^n} \quad . \tag{A.3}$$

Defining

$$\mu \frac{\partial}{\partial \mu} g = -\frac{\varepsilon}{2} g + \beta(g) \tag{A.4}$$

and

$$\gamma_m = \frac{\mu}{m}\frac{\partial}{\partial\mu} m \qquad (A.5)$$

we have

$$[\mu\frac{\partial}{\partial\mu}+\beta(g)\frac{\partial}{\partial g}+\gamma_m m\frac{\partial}{\partial m}]\Pi(q^2,g^2,m,\mu) = [\varepsilon+\left(\varepsilon/2-\beta(g)\right)\frac{\partial}{\partial g}]\sum_{n=1}^{\infty}\frac{C_n(g)}{\varepsilon^n} \quad . \qquad (A.6)$$

The left-hand-side is finite, so we obtain

$$[\mu\frac{\partial}{\partial\mu}+\beta(g)\frac{\partial}{\partial g}+\gamma_m m\frac{\partial}{\partial m}]\Pi(q^2,g^2,m,\mu) = \frac{\partial}{\partial g}g^2 C_1(g) \equiv D(g) \quad , \qquad (A.7)$$

and

$$\frac{\partial}{\partial g^2}[g^2 C_{n+1}(g)] = \beta(g)\frac{\partial}{\partial g}C_n(g) \quad . \qquad (A.8)$$

The second relation just reflects the well-known fact that the leading divergences in each order are determined in terms of lower order calculations. It appears explicitly, for example, in the calculation of Dine and Sapirstein.[4]

For simplicity we consider massless quarks in the rest of this section. Equation (A.7) is readily integrated using the running coupling constant. With $\eta \equiv \ell n(-q^2/\mu^2)$ we define

$$\frac{\partial}{\partial\eta}\bar{g}(\eta) = \beta(\bar{g}) \quad . \qquad (A.9)$$

The first two terms on the right-hand side are known, and are independent of renormalization convention.

Writing

$$\beta(g) = -\beta_0 \frac{g^3}{16\pi^2} - \beta_1 \frac{g^5}{(16\pi^2)^2} \tag{A.10}$$

we have

$$\beta_0 = \frac{11}{3} C_A - \frac{2}{3} N_f \tag{A.11}$$

$$\beta_1 = \frac{34}{3} C_A^2 - \frac{10}{3} C_A N_f - 2 C_f N_f \tag{A.12}$$

where C_A and C_F are the quadratic Casimir operators for the adjoint and fermion representations, respectively, and N_f is the number of flavors $\left(\text{for SU(N), } C_A = N, C_F = (N^2-1)/2N\right)$. Defining $\left[\alpha_s(q^2) \equiv \left(g^2(\eta)/4\pi\right)\right]$,

$$\alpha_s^0(q^2) \equiv \frac{4\pi}{\beta_0 \ln(-q^2/\Lambda^2)} \tag{A.13}$$

one may write, with an appropriate definition of Λ,

$$\alpha_s(q^2) = \alpha_s^0(q^2)\left(1 - \alpha_0^s(q^2) \frac{\beta_1}{4\pi\beta_0} \ln\ln(-q^2/\Lambda^2)\right) + \mathcal{O}(\alpha_s^3) \quad . \tag{A.14}$$

Note that, to determine Λ, one must keep all terms in a given process to order α_0^2. To see this, note under the rescaling $\Lambda \to \Lambda' = a\Lambda$, $\alpha_s^0(q^2) \to \alpha_s^{0'} + (\beta_0/4\pi) \ln(a)(\alpha_s^{0'})^2$. In terms of $\bar{g}(t)$, the solution of (A.7) is

$$\Pi(\bar{q}^2) = \Pi(\bar{g}(\eta), q_0^2, m) - \int_0^\eta D\left(\bar{g}(\eta')\right) d\eta' \quad . \tag{A.15}$$

Using well known QED results[35] and the results of the second order calculation, we have

$$C_1(g^2) = -\frac{2}{3} - \frac{1}{4} C_F \frac{g^2}{4\pi^2} + C_F \left[B + \beta_0/8(L - 4D)\right] (g^2/4\pi^2)^2 + \mathcal{O}(g^6) \tag{A.16}$$

where

$$B = 0.212\ C_F - 0.0506\ C_A + 0.00579\ N_f \qquad (A.17)$$

$$D = 0.0564 \qquad (A.18)$$

and L reflects the freedom to make finite renormalizations of the coupling constant. In particular, the $\overline{MS}$ scheme, due to Bardeen et al.,[2] tends to yield small results for higher order corrections, and is defined by

$$L = (\ell n\ 4\pi - \gamma)/2 \qquad (A.19)$$

where γ is Euler's constant. It is now a straightforward matter to evaluate the right-hand side of Eq. (A.15). The result can be used as input for dispersive analyses. Taking its discontinuity to obtain R gives Eq. (2.1) for large s.

For including finite mass effects in first order in α_s, an "on-shell" definition of the quark mass is convenient. Such a scheme is discussed, for example, by De Rújula and Georgi.[14] In this scheme, the β-function and the running coupling constant depend on the quark masses. Such a definition is used in the text when effects of the charmed quark mass are included.

REFERENCES

1. H. D. Politzer, Phys. Rev. Lett. 30, 1346 (1973); D. J. Gross and F. Wilczek, Phys. Rev. Lett. 30, 1343 (1973), Phys. Rev. D8, 3633 (1973) and D9, 980 (1974); A. Zee, F. Wilczek and S. B. Treiman, Phys. Rev. D10, 2881 (1974); H. Georgi and H. D. Politzer, Phys. Rev. D9, 416 (1974); S. Weinberg, Phys. Rev. Lett. 31, 494 (1973).

2. W. A. Bardeen, A. J. Buras, D. W. Duke and T. Muta, Phys. Rev. D18, 3998 (1978).

3. E. G. Floratos, D. A. Ross and C. T. Sachradja, Nucl. Phys. B129, 66 (1977) [erratum: B139, 545 (1978)], Nucl. Phys. B152, 493 (1979) and Phys. Lett. 80B, 269 (1979); W. A. Bardeen and A. J. Buras, Phys. Lett. 86B, 61 (1979).

4. M. Dine and J. Sapirstein, Phys. Rev. Lett. 43, 668 (1979); K. G. Chetyrkin, A. L. Kataev and F. V. Tkachev, Phys. Lett. 85B, 277 (1979); W. Celmaster and R. J. Gonsalves, University of California at San Diego, Report No. 10 P10-206 (1980).

5. M. Bacé, Phys. Lett. 78B, 132 (1978).

6. L. F. Abbott and R. M. Barnett, Stanford Linear Accelerator Center SLAC-PUB-2325 (May 1979), to be published in Ann. Phys. (N.Y.); L. F. Abbott, W. B. Atwood and R. M. Barnett, Stanford Linear Accelerator Center SLAC-PUB-2400 (Sept. 1979).

7. All Mark I data used are from: J. Siegrist, Stanford Linear Accelerator Center Report No. SLAC-225 (1979), except where better data exist from the "lead-glass-wall" collaboration (of Mark I): P. Rapidis et al., Phys. Rev. Lett. 39, 526 and 974 (1977); see also R. F. Schwitters, in Proc. 1975 Int. Symposium on Lepton-Photon Interactions at High Energies, ed. W. T. Kirk (Stanford Linear Accelerator Center, Stanford University, Stanford, California, 1975), p.5; J. Siegrist et al., Phys. Rev. Lett. 36, 700 (1976). Data from other low-energy experiments: E. D. Bloom et al. (Crystal Ball), Stanford Linear Accelerator Center SLAC-PUB-2425 (Nov. 1979); J. Kirkby (DELCO) private communication; Ch. Berger et al. (PLUTO), Phys. Lett. 81B, 410 (1979); R. Brandelik et al. (DASP), Phys. Lett. 76B, 361 (1978); references to data below $\sqrt{s}$ = 3 GeV are contained in C. Bacci et al., Phys. Lett. 86B, 234 (1979).

8. All PETRA data in Fig. 9 will appear in the Proc. of the 9th Int. Symposium on Lepton and Photon Interactions at High Energies, Batavia, Illinois, August 23-29 (1979). See also [JADE]: W. Bartel et al., Phys. Lett. 88B, 171 (1979); S. Orito et al., Report No. DESY 79/77 (Nov. 1979); and [TASSO]: R. Bradelik et al., Report No. DESY-79/74 (Nov. 1979) and Phys. Lett. 83B, 261 (1979); G. Wolf et al., Report No. DESY-79/61 (Sept. 1979); [Mark J]: D. P. Barber et al., Phys. Lett. 85B, 463 (1979), Phys. Rev. Lett. 43, 901 (1979) and Phys. Rev. Lett. 42, 1113 (1979); [PLUTO]: Ch. Berger et al., Phys. Lett. 86B, 413 (1979), Phys. Lett. 81B, 410 (1979) and Report No. PITHA 79/29 (Oct. 1979).

9. F. J. Yndurain, Nucl. Phys. B136, 533 (1978); F. A. Berends and G. J. Komen, Phys. Lett. 63B, 432 (1976) and Nucl. Phys. B115, 114 (1976).

10. T. Appelquist and H. Georgi, Phys. Rev. D8, 4000 (1973); A. Zee, Phys. Rev. D8, 4038 (1973).

11. M. Gell-Mann and F. E. Low, Phys. Rev. 95, 1300 (1954).

12. W. E. Caswell, Phys. Rev. Lett. 33, 244 (1974); D. R. T. Jones, Nucl. Phys. B75, 531 (1974).

13. See the review by A. J. Buras, Report No. Fermilab-Pub-79/17-Thy (1979).

14. S. L. Adler, Phys. Rev. D10, 3714 (1974); A. De Rújula and H. Georgi, Phys. Rev. D13, 1296 (1976).

15. K. Wilson, Phys. Rev. 179, 1499 (1969); W. Zimmermann, in Lectures in Elementary Particles and Quantum Field Theory, eds. S. Deser, M. Grisaru and H. Pendleton (MIT Press, Cambridge, Massachusetts, 1970).

16. M. A. Shifman, A. I. Vainshtein and V. I. Zakharov, Nucl. Phys. B147, 389, 448 and 519 (1979).

17. J. Schwinger, Particles, Sources and Fields, Vol. II (Addison-Wesley, New York, 1973), Chaps.4 - 5.

18. E. C. Poggio, H. R. Quinn and S. Weinberg, Phys. Rev. D13, 1958 (1976); R. Shankar, Phys. Rev. D15, 755 (1978).

19. C. Bricman et al., "Review of Particle Properties," Report No. LBL-100 (1978); H. Meyer, Report No. DESY 79/81 (Dec. 1979), to be published in Proceedings of the 9th Int. Symp. on Lepton and Photon Interactions at High Energies, Batavia, Illinois, Aug. 23-29, 1979.

20. J. Siegrist, Report No. SLAC-225 (1979).

21. Private communication G. J. Feldman.

22. For 2-prong events see Fig. 32 in J. Siegrist, Report No. SLAC-225 (1979); for μe events see Fig. 4 in M. L. Perl, Report No. SLAC-PUB-2446 (1979), and M. L. Perl, private communication.

23. W. Bacino et al., Phys. Rev. Lett. 41, 13 (1978).

24. D. P. Barber et al., Phys. Rev. Lett. 43, 1915 (1979).

25. G. S. LaRue et al., Phys. Rev. Lett. 38, 1011 (1977); Phys. Rev. Lett. 42, 142 (1979), [erratum: Phys. Rev. Lett. 42, 1019 (1979)].

26. R. N. Cahn, Phys. Rev. Lett. 40, 80 (1978); Y. J. Ng and S. H. H. Tye, Phys. Rev. Lett. 41, 6 (1978); H. Georgi and S. L. Glashow, Nucl. Phys. B159, 29 (1979); F. Wilczek and A. Zee, Phys. Rev. D16, 860 (1977); H. Fritzsch, Phys. Lett. 78B, 611 (1978); P. G. O. Freund and C. T. Hill, Phys. Rev. D19, 2755 (1979).

27. L. N. Chang and J. E. Kim, Phys. Lett. 81B, 233 (1979); J. F. Donoghue and L. F. Li, Phys. Rev. D19, 945 (1979); C. H. Albright, J. Smith and S. H. H. Tye, Report No. Fermilab-Pub-79/69-Thy (Sept. 1979); G. L. Kane, Report No. SLAC-PUB-2326 (1979).

28. G. Altarelli, R. K. Ellis and G. Martinelli, Nucl. Phys. B157, 461 (1979).

29. R. G. Moorhouse, M. R. Pennington and G. G. Ross, Nucl. Phys. B124, 285 (1977).

30. M. Piccolo et al., Phys. Rev. Lett. 39, 1503 (1977).

31. T. Appelquist and R. Shankar, Phys. Rev. D18, 2952 (1978); N. Andrei and D. J. Gross, Phys. Rev. D18, 468 (1978); L. Baulieu et al., Phys. Lett. 77B, 290 (1978).

32. V. Novikov, L. Okun, M. Shifman, A. Vainshtein, M. Voloshin and V. Zakharov, Phys. Rep. 41C, 1 (1978).

33. G. 't Hooft, Nucl. Phys. B62, 444 (1973).

34. G. 't Hooft and M. Veltman, Nucl. Phys. B44, 189 (1972).

35. R. Jost and J. M. Luttinger, Helv. Phys. Acta. 23, 201 (1950).

TABLE I

Estimates of the Uncertainties in the Theoretical Calculation of R [a]

Source	Magnitude of Uncertainties	
	$\sqrt{s}$ = 3 - 5 GeV	$\sqrt{s} \gtrsim 5$ GeV
Uncertainty in value of Λ	4%	2%
Uncertainty in value of m_c	10% [b] 0.1% [c]	< 0.1%
QCD effects beyond the calculated order [d]	5%	1%
Higher-order QED effects	0.2%	0.2%
Uncertainty inherent in the smearing technique	1%	1%

[a] More specific remarks appear in the text.

[b] Magnitude of uncertainty for $\sqrt{s} \approx 3$ GeV.

[c] Magnitude of uncertainty for $\sqrt{s} \gtrsim 4.1$ GeV.

[d] This item encompasses non-perturbative corrections, higher-twist effects, running-mass effects, etc.

FIGURE CAPTIONS

1. Feynman diagram for heavy quark production which diverges as $1/v$ near threshold. Wavy lines represent photons; spiral lines represent gluons.

2. Integration contour C for Eq. (2.19).

3. Integration contour C' for $\overline{R}(s)$. Δ is chosen sufficiently large that $\Pi(s)$ may be evaluated along C' using perturbation theory.

4. Vacuum polarization insertion to the virtual photon line.

5. Electron loop contribution to vacuum polarization.

6. Born contribution to the annihilation cross section.

7. Diagrams contributing to the Bhabha cross section involving vacuum polarization loops.

8. Data for R from the SLAC-LBL collaboration (Ref. 7). In our work we used smaller bins in the resonance region. The contribution of the τ has been subtracted, and radiative corrections have been applied. Only statistical errors are shown. The locations of J/ψ and ψ' have been indicated, since they are included in determining the charm threshold. The curve is the QCD prediction for R with $\Lambda = 0.45$ GeV (see discussion of QED corrections in text).

9. All data (Refs. 7 and 8) for R above the charm resonance region are shown. The contribution of τ has been subtracted, and radiative corrections have been applied. Error bars are statistical only and neglect 10 - 15% systematic uncertainties. Data around $\sqrt{s}$ = 30 GeV are placed together in large bins as are all Mark I data. The resonance region is drawn crudely, and some data below that region are also shown. The location of J/ψ, ψ', Υ and Υ' are also shown, since they determine c and b thresholds. The QCD calculations for R for several values of Λ are given. $\Lambda = 0$ indicates the results of the quark-parton model ($\alpha_s = 0$).

10. A comparison of the results of smearing theoretical and experimental values of R using two different weighting functions. In both cases $\Delta = 5$ GeV^2 and $\Lambda = 0.45$ GeV (for the QCD curves). The SLAC-LBL (Mark I) data are from Ref. 7. In the resonance region the data bins are too close together to show individually, so we have shaded them instead. (a) uses the Gaussian weighting function, Eq. (4.6). (b) uses the power-law weighting function, Eq. (4.5), of Poggio, Quinn and Weinberg.[18]

11. The results of smearing the theoretical and experimental values of R with the Gaussian weighting function of Eq. (4.6) with $\Delta = 5$ GeV^2. The SLAC-LBL (Mark I) data used are from Ref. 7. In the resonance region the data bins are too close together so show individually, so we have shaded them instead. The error bars shown are statistical only. The curves are QCD for several values of Λ. $\Lambda = 0$ indicates the quark-parton model ($\alpha_s = 0$).

12. The results of smearing the theoretical and experimental values of R as in Fig. 11. The theory curve represents QCD when a hypothetical charge -1/3 quark of mass 3 GeV is included ($\Lambda = 0.45$ GeV).

13. The slopes ($d\overline{R}/d\sqrt{s}$) of the $\Lambda = 0.45$ GeV curves for $\overline{R}$ in Figs. 11 and 12. The data are represented by the dotted curve (where error bars have been omitted for clarity). The QCD curves are shown with and without the hypothetical charge -1/3 quark of mass 3 GeV.

14. A comparison of theoretical and experimental values of R as in Fig. 8. The theoretical curve represents QCD when the full contribution of a hypothetical lepton of integer charge and mass 2.85 GeV is included ($\Lambda = 0.45$ GeV). It is not necessary to smooth R at high energies since the lepton does not have QCD corrections; the smoothed R plot closely resembles this plot for $\sqrt{s} > 5$ GeV.

15. The results of smearing the theoretical and experimental values of R as in Fig. 11. The theory curve represents QCD when two hypothetical charged Higgs bosons of mass 2 GeV are included ($\Lambda = 0.45$ GeV).

16. The results of smearing the theoretical and experimental values of R as in Fig. 11. The theory curve represents QCD when hypothetical form-factor and constituents are assigned to the charm quark ($\Lambda = 0.45$ GeV).

17. Diagrams contributing to $\Pi_{\mu\nu}$: (a) lowest-order term (quark-model result), (b) order g^2 corrections and (c) examples of order g^4 corrections.

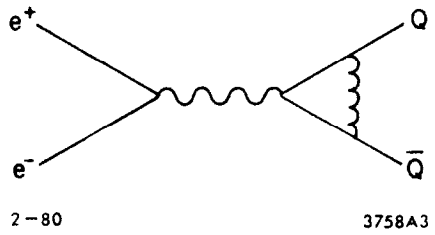

Fig. 1

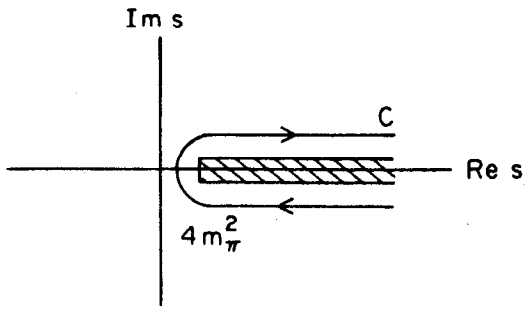

Fig. 2

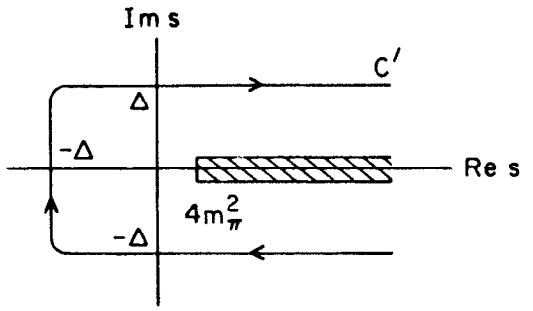

Fig. 3

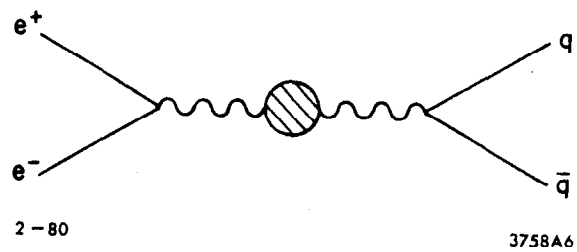

Fig. 4

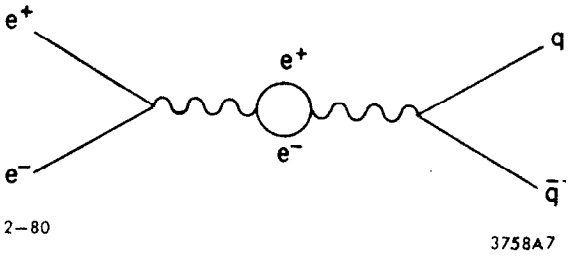

Fig. 5

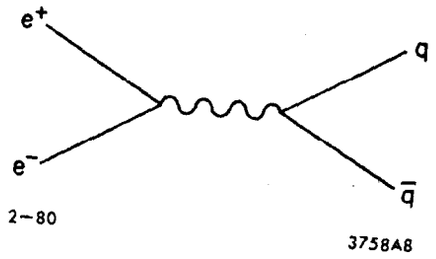

Fig. 6

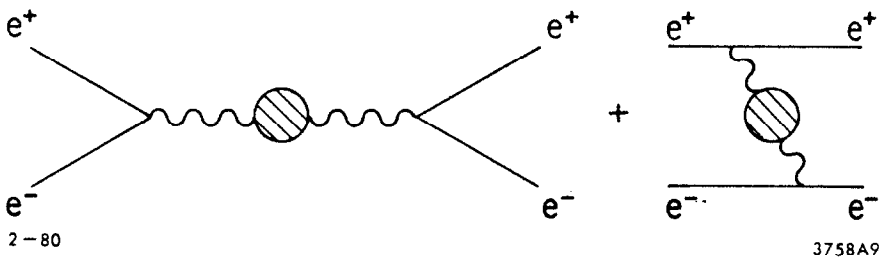

Fig. 7

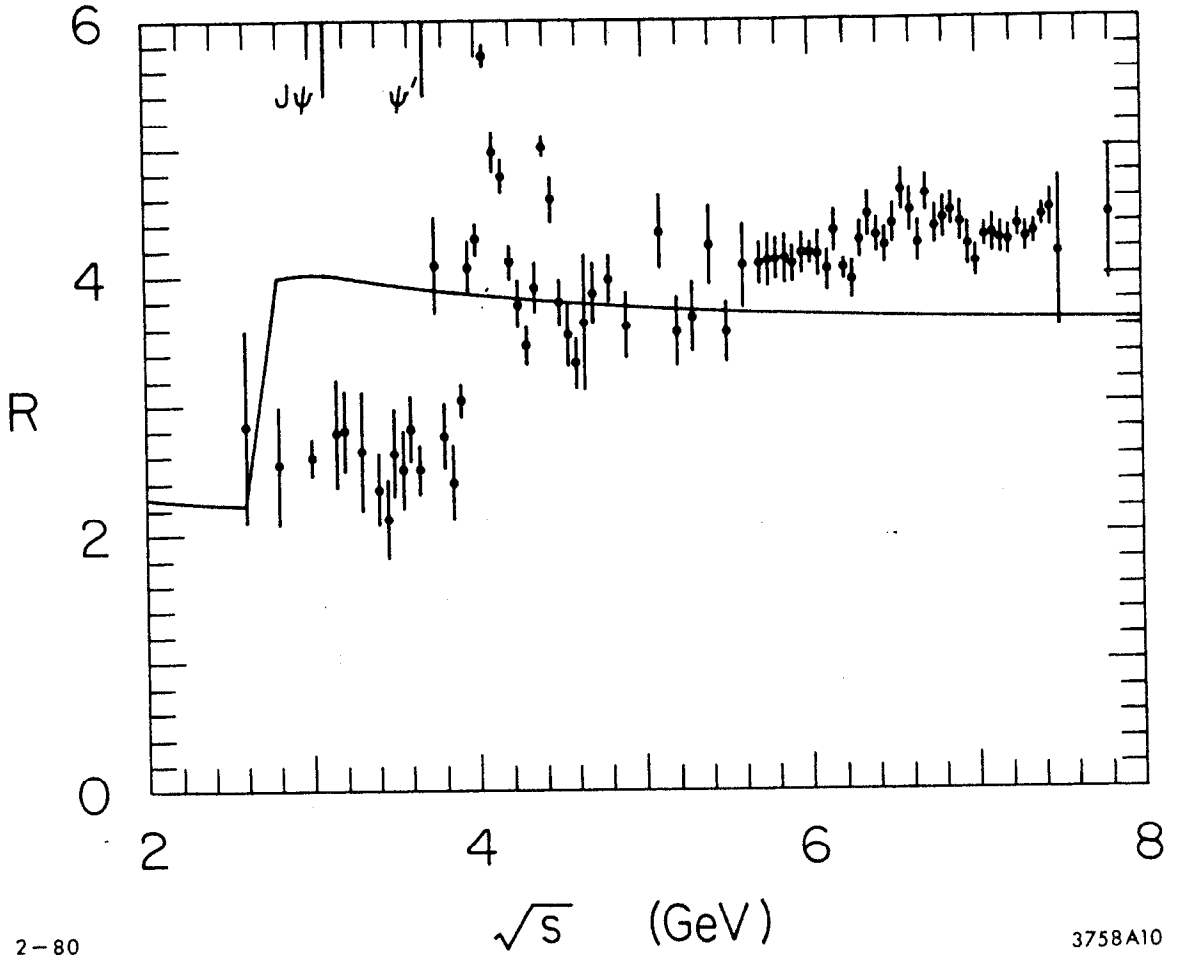

Fig. 8

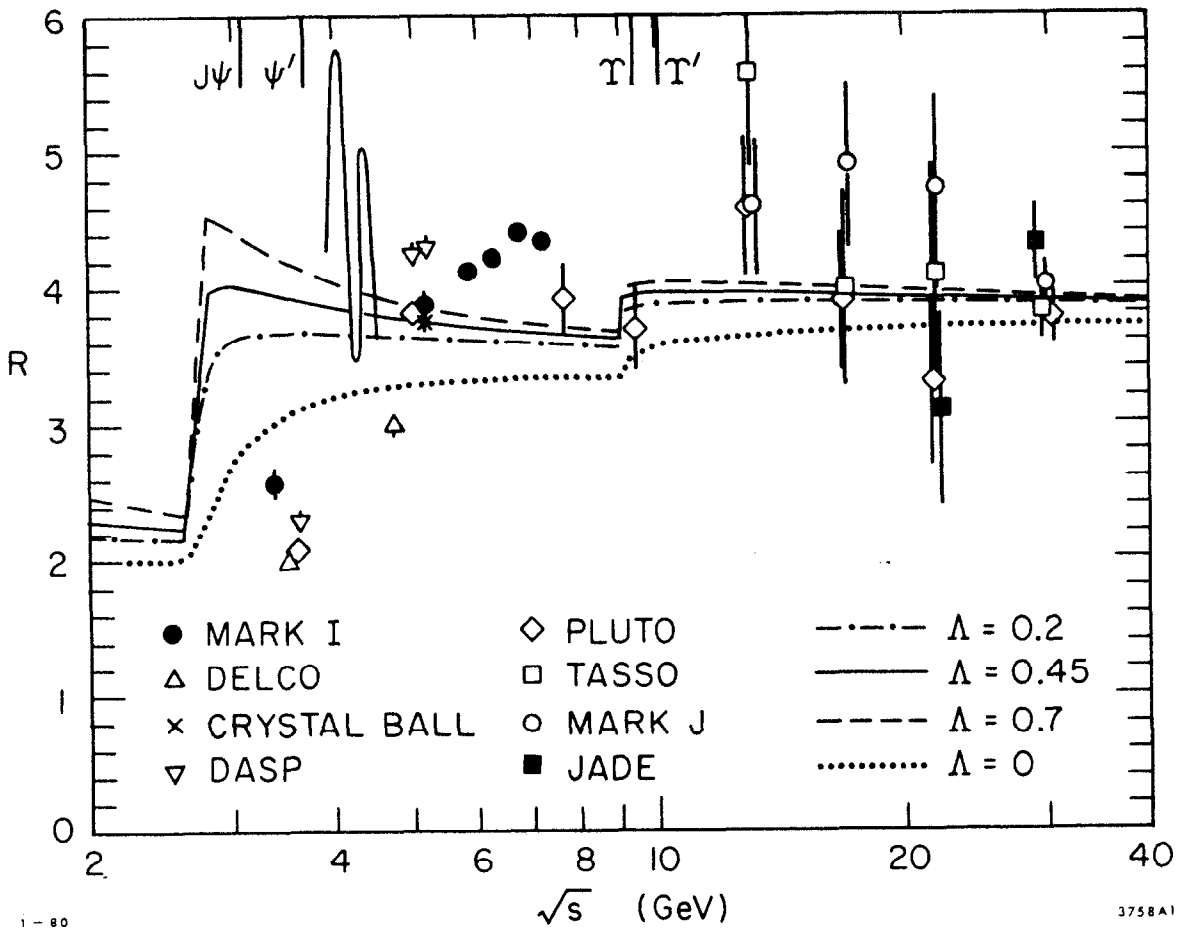
6
5
4
3
2
1
0
R
Jψ
ψ′
ϒ
ϒ′
MARK I
DELCO
CRYSTAL BALL
DASP
PLUTO
TASSO
MARK J
JADE
Λ = 0.2
Λ = 0.45
Λ = 0.7
Λ = 0
2
4
6
8
10
20
40
√s (GeV)
1-80
3758A1

Fig. 9

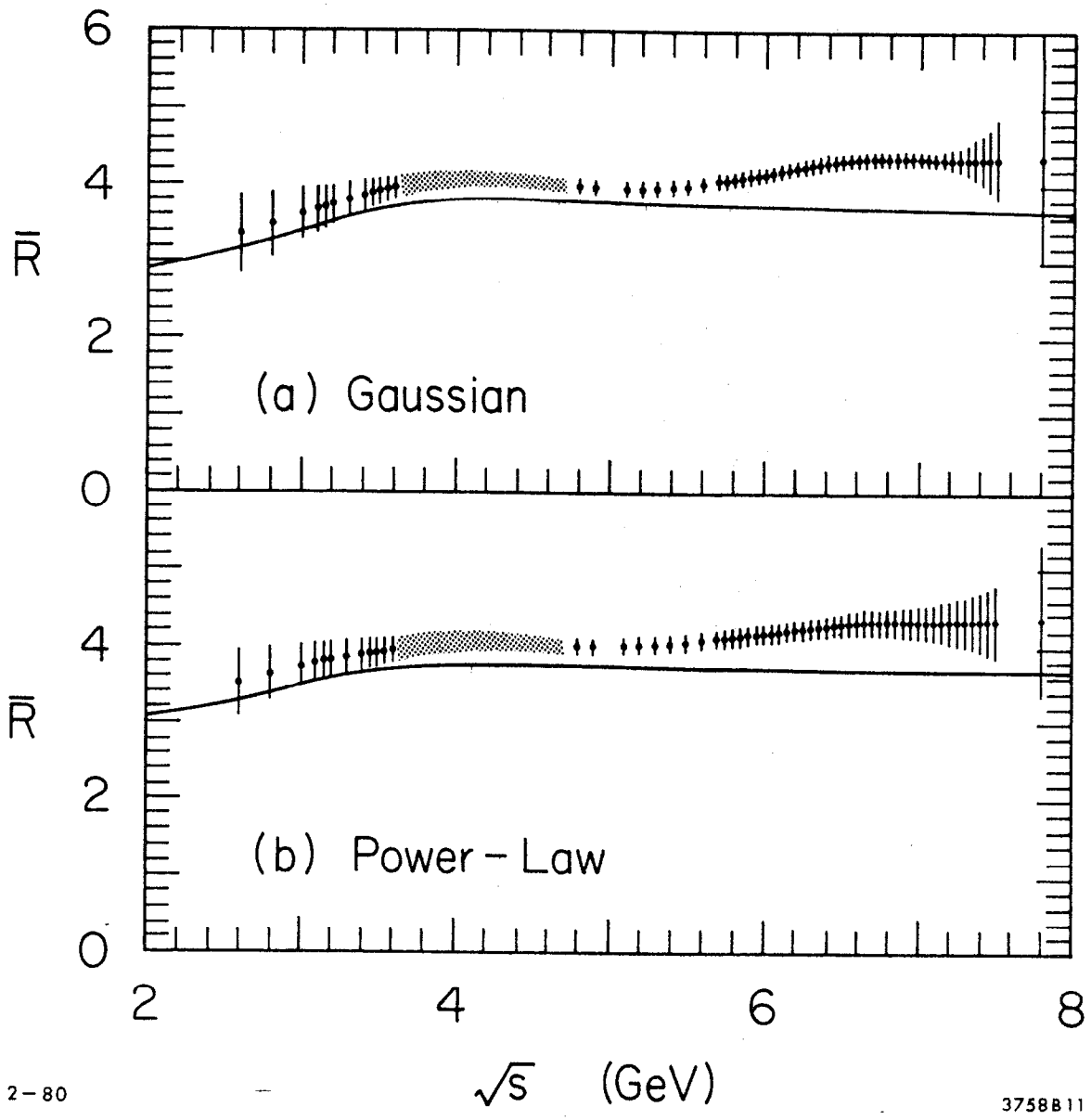

Fig. 10

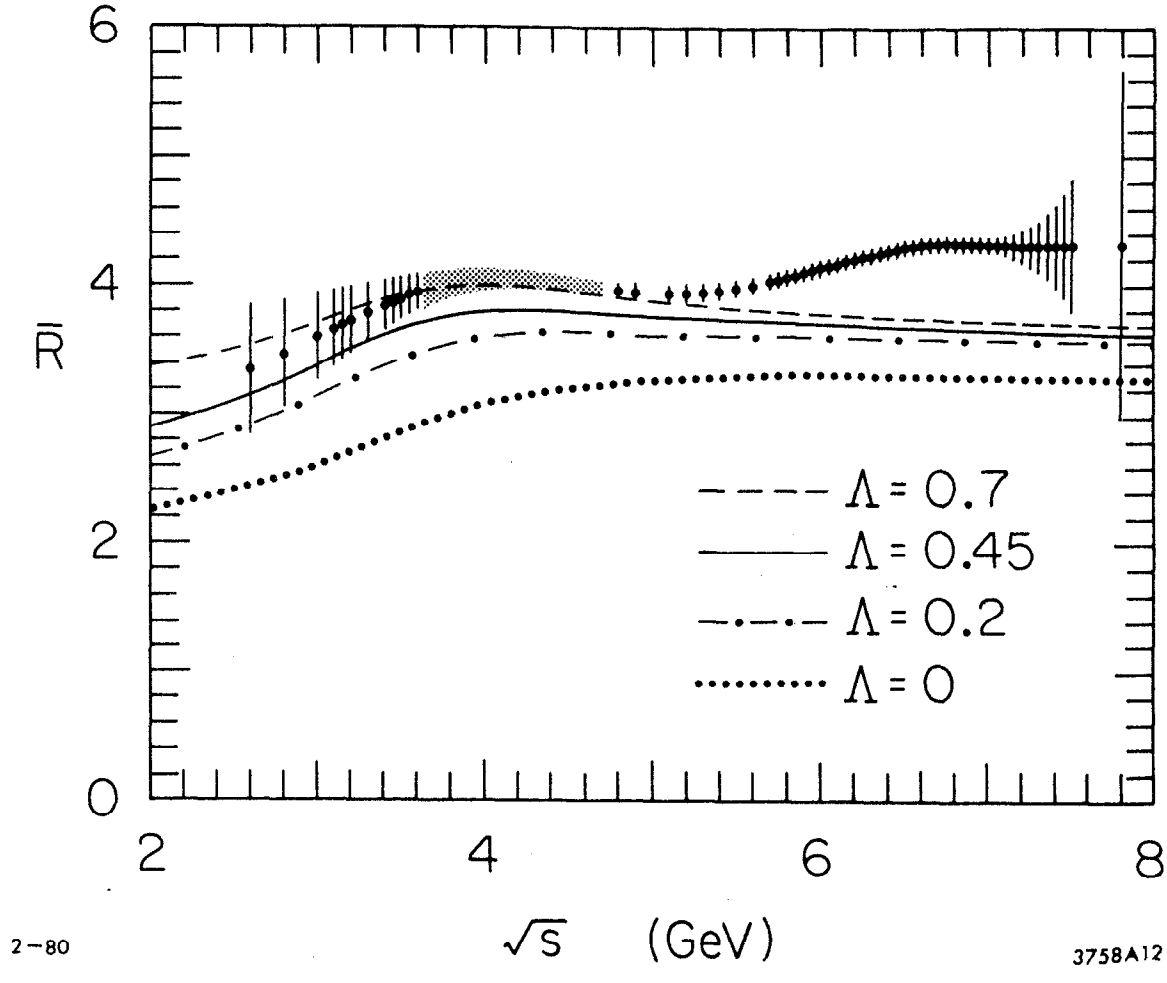

Fig. 11

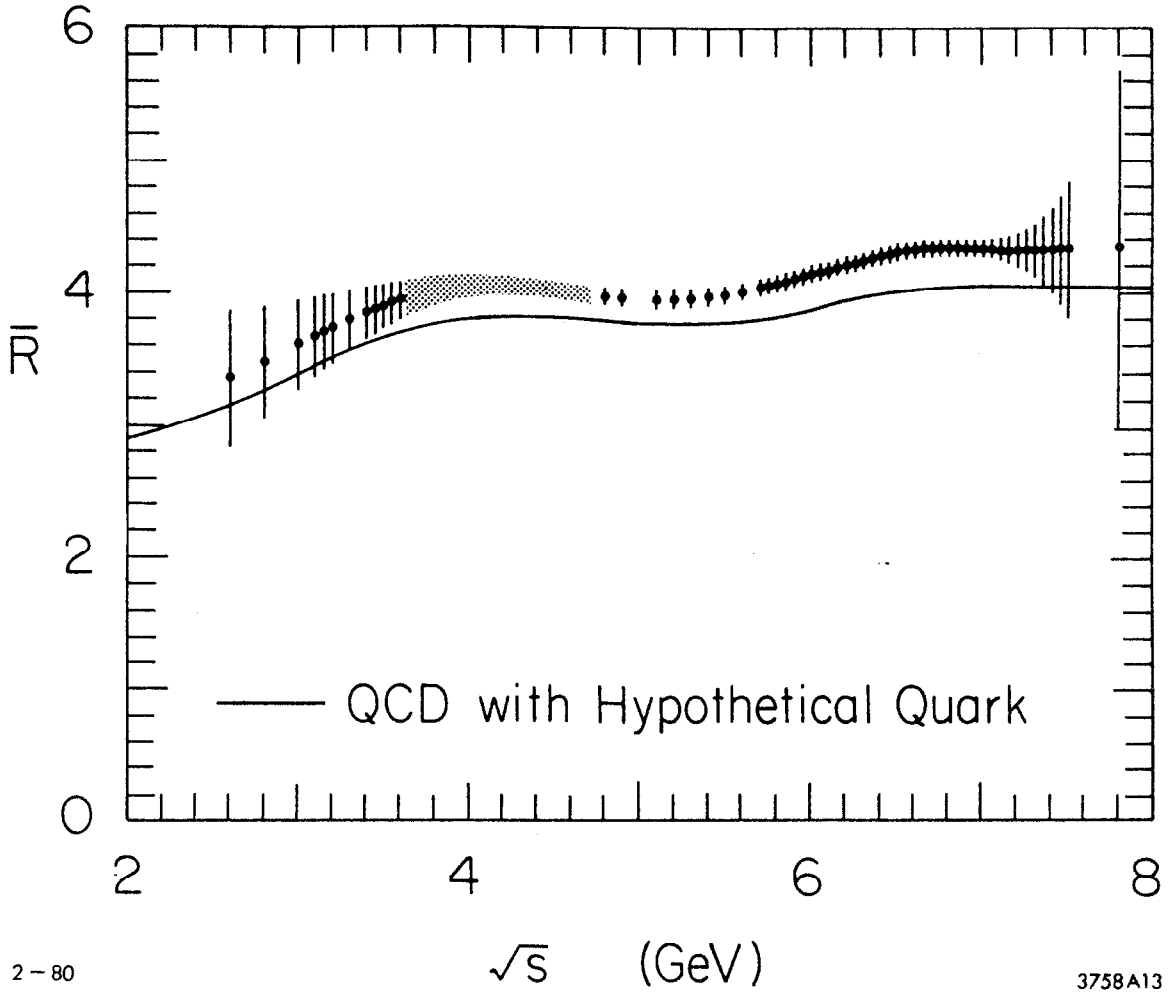
6
4
2
0
$\bar{R}$
QCD with Hypothetical Quark
2
4
6
8
$\sqrt{s}$ (GeV)
2 – 80
3758A13

Fig. 12

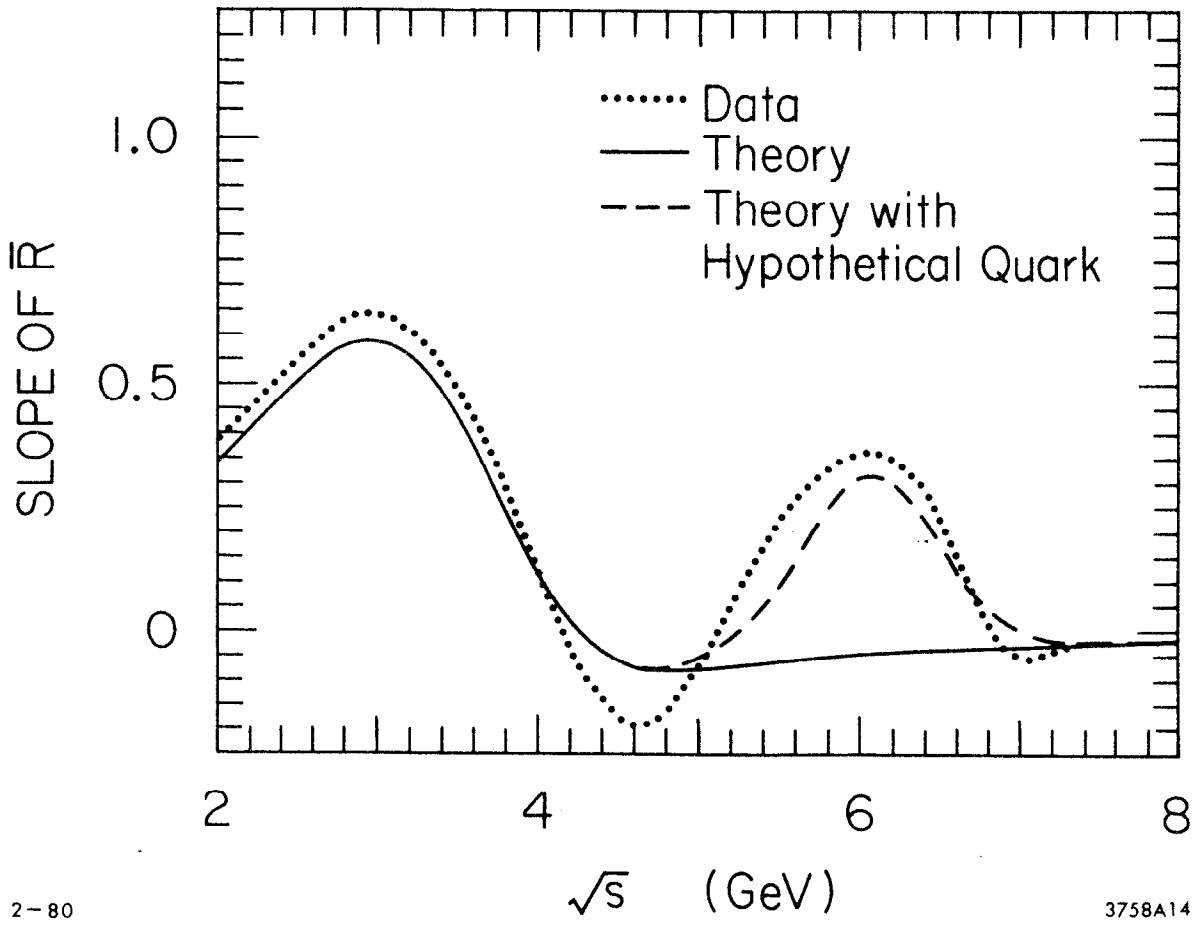
Data
Theory
Theory with
Hypothetical Quark
SLOPE OF R
1.0
0.5
0
2
4
6
8
√s (GeV)
2-80
3758A14

Fig. 13

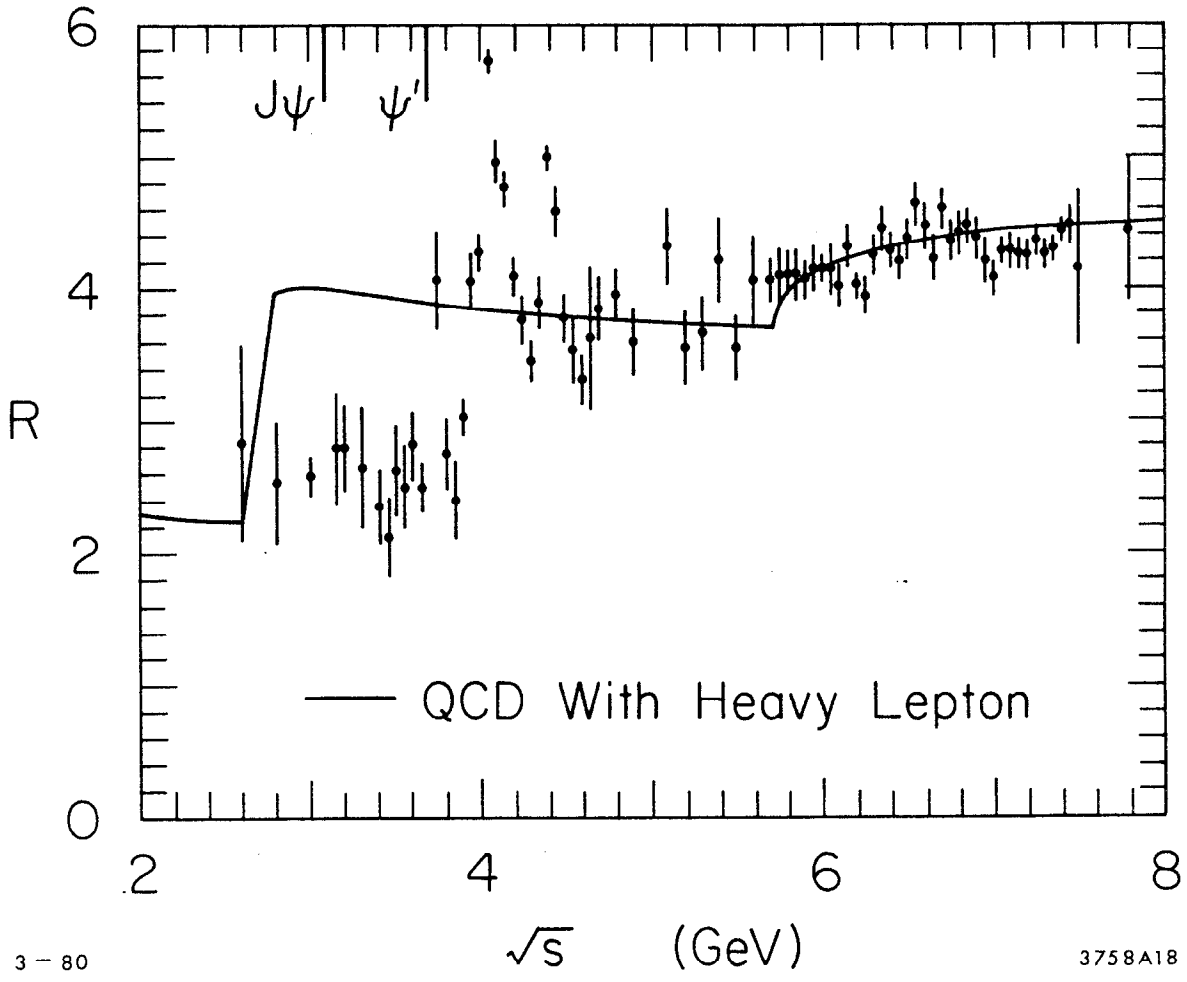

Fig. 14

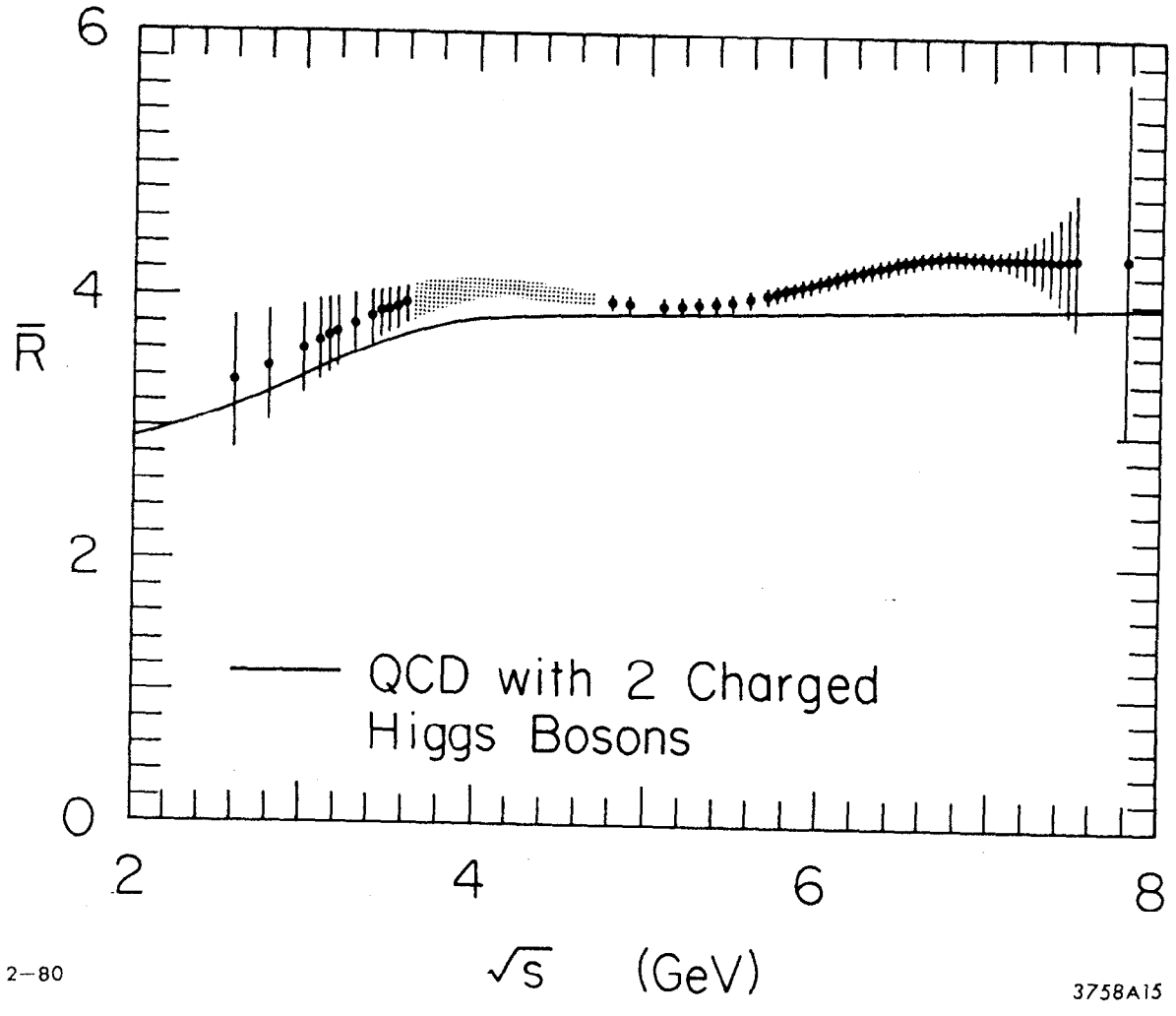
6
4
2
0
$\bar{R}$
QCD with 2 Charged
Higgs Bosons
2
4
6
8
$\sqrt{s}$ (GeV)
2-80
3758A15

Fig. 15

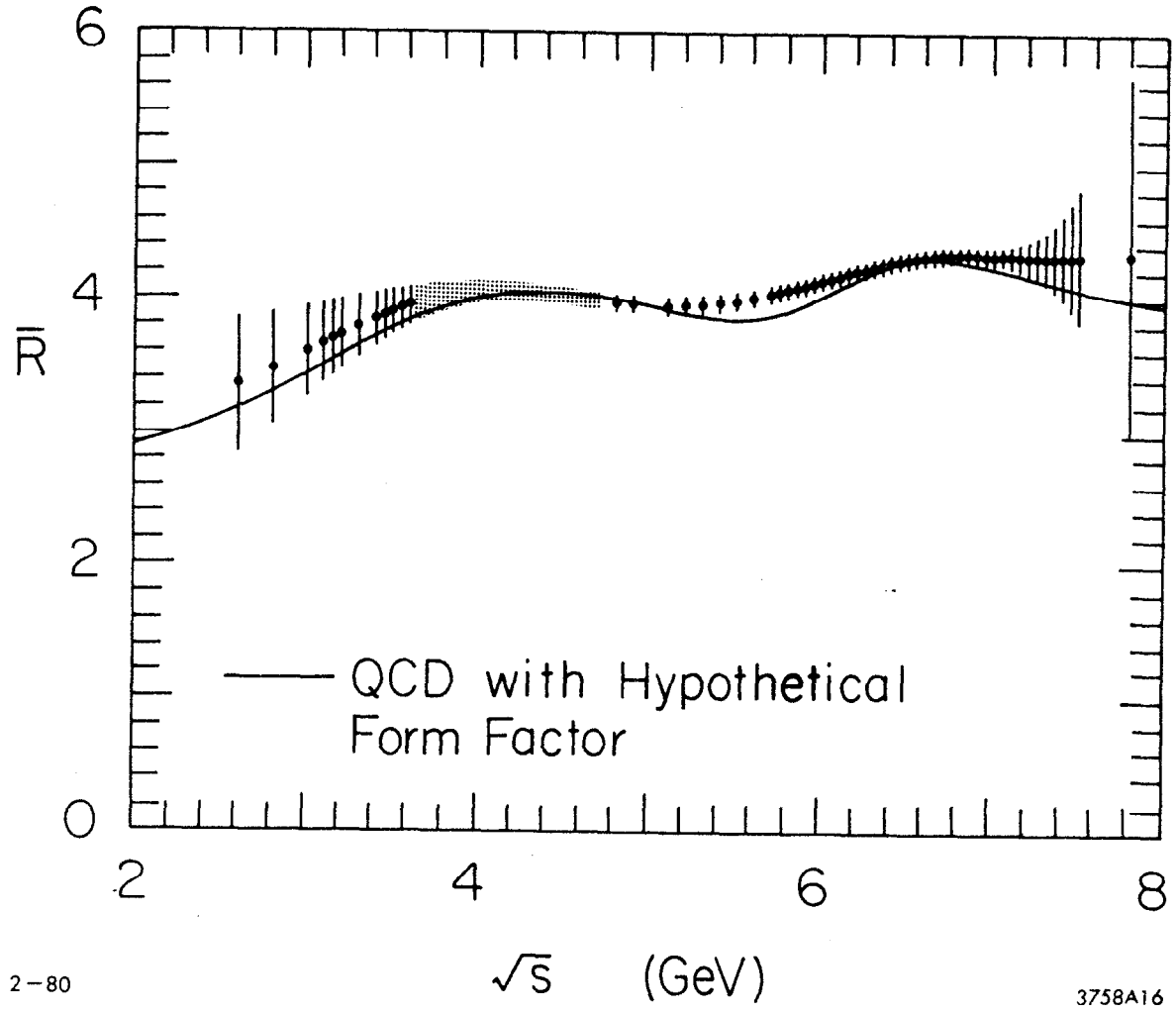
6
4
2
0
R
2
4
6
8
QCD with Hypothetical
Form Factor
√s (GeV)
2-80
3758A16

Fig. 16

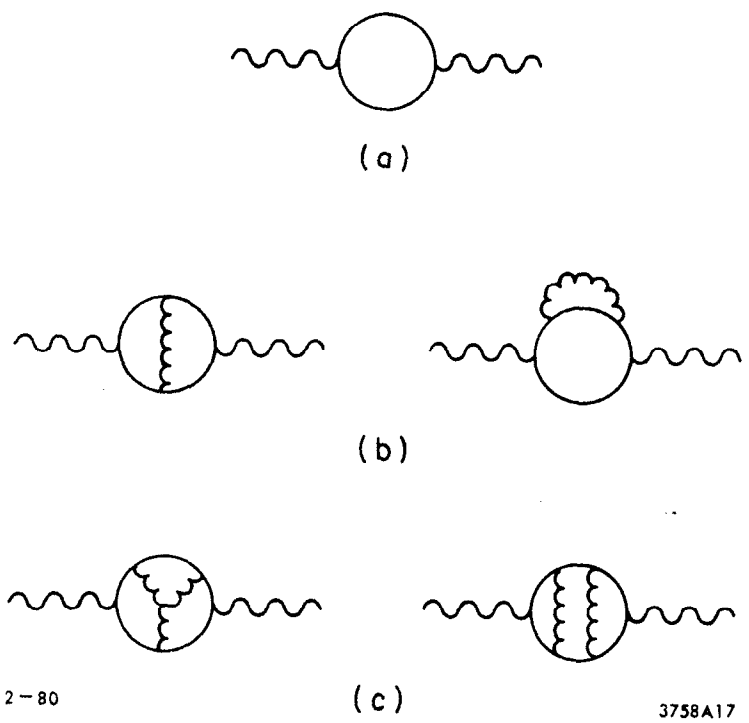

Fig. 17